

1. Title- Gemcitabine Loaded Galactosylated Albumin Nanoparticles for the Effective Treatment of Hepatocellular Carcinoma

2. Introduction

Cancer is a primary cause of the increased mortality rate worldwide. According to WHO report 2020, around 10 million individuals died due to cancer among which 0.8 million individuals experienced the lethality of hepatocellular carcinoma (HCC). HCC is the fourth most cause of mortality worldwide (**WHO Report, 2020**)¹. The increased incidences of deaths are observed due to delayed prognosis. The ‘Ashwell–Morell Receptor’ commonly referred to as asialoglycoprotein receptors, ASGPR are the receptors primarily over-expressed on the periphery of hepatocytes. In several studies, ASGPR-specific carriers were developed but few limitations were consistently observed such as instability of cargoes in the body fluid, intricacy in carrier modification, drug inactivation, rapid elimination, biodegradation etc. A broad spectrum of molecules exhibiting galactose or its derivatives at the terminal position has a higher affinity towards the ASGPR receptor for the internalization of the molecules (**Morell et al., 1968**)². Hence, the concept of galactosylation can be an asset in the effective targeting of ASGPR on the hepatocytes and in turn for the HCC. This approach was initially maneuvered in 1968 to treat HCC by showcasing an inhibitory effect on DNA synthesis (**O’Hare et al., 1989**)³.

Lactobionic acid (LA), a disaccharide constituted by the glycosidic linkage between D-gluconic acid, and β -D-galactose. Numerous research studies indulging LA and its derivatives have been explored in distinct areas such as pharmaceuticals, cosmeceuticals, and nutraceuticals (**FDA-NDA Review and Evaluation, 2011**)⁴. It is commonly employed as a ligand for the treatment of liver associated diseases due to its binding ability with the ASGPR receptors. ASGPR receptors are over-expressed on the surface of metastatic hepatocytes. The binding of LA on ASGPR receptors assist in the internalization of drugs using different nanocarrier systems. **Pan et al.** have reported the doxorubicin-loaded LA conjugated nanosystem as a promising candidate for the treatment of hepatic cancer and has nicely explained the concept of selective recognition by LA (**Pan et al., 2016**)⁵.

Nanocarriers like liposomes, nanoparticles, micelles, etc have captivated the attention of various research groups towards cancer therapy (**Ruman et al., 2020**)⁶. Among various nanocarriers, nanoparticles (NPs) are the oldest and commonly used carriers for the effective

drug delivery. Their usual size is between 1-1000 nm. The potency and efficacy of the drug may be enhanced as well as secured by taking advantage of NPs as a carrier system (**Bayda et al., 2019**)⁷. Currently, serum albumin NPs are considered as the most potent carrier system for the targeting of biomarkers, drugs, or any other bio-actives. Serum albumins such as human serum albumin (HSA) and bovine serum albumin (BSA) are natural homologous proteins, usually preferred for achieving an effective targeting of a drug in the form of nanoformulations.

In 2005, the first BSA NPs were commercialized under the trade name of Abraxane (nab-paclitaxel) by American Biosciences, Inc. for the treatment of breast cancer followed by lung cancer (2007), and adenocarcinoma (2013) (**American BioSciences Inc., 2013**)⁸. The BSA NPs are utilized to facilitate the endothelial transcytosis of albumin-bound or unbound plasma constituents to the extracellular matrix. The drug can be loaded into the BSA protein matrix *via* covalent or non-covalent conjugation. The amino group and carboxylic functionality on BSA are utilized for conjugating the drug molecules covalently, henceforth, pertains to the stability of the formulation (**Wang et al., 2018**)⁹. For an instance, Song *et al.* elaborated the polymerization of polypyrrole and covalently conjugating it with BSA derivative to formulate an efficacious nanoformulation for the suggested cancer therapy (**Song et al., 2015**)¹⁰. In 2017, Kushwah *et al.* have fabricated gemcitabine conjugated BSA NPs (GEM-BSA NPs) using high-pressure homogenization technique to potentiate drug efficacy in pancreatic adenocarcinoma. It was observed that the GEM-BSA NPs were developed by a covalent conjugation between succinylated-GEM and free-amine terminated BSA. The GEM-BSA NPs assisted in the alteration of physicochemical characteristics of GEM by potentiating the therapeutic efficacy, stability, and cell uptake *via* clathrin-mediated pathway (**Kushwah et al., 2017**)¹¹. Effective conjugation may result into the modification of physicochemical characteristics of GEM.

GEM is a broad-spectrum anti-neoplastic agent that has been approved by USFDA for the treatment of various types of malignancies such as advanced pancreatic adenocarcinoma, lung cancer, breast cancer, and ovarian cancer in the year 1996, 1998, 2004, and 2006 respectively (**USFDA Report, 2010**)¹². In therecent studies, GEM has also been exploredfor the treatment of hepatocellular carcinoma (HCC)as a stand-alone or combinatorial therapeutic agentwhich pertains several limitations such as short half-life, rapid bioconversion into inactive metabolite (2',2'-difluorodeoxyuridine (dFdU)) after i.v. administration, low protein binding, less permeation, reduced clinical efficacy and targetability (**Martín-Banderas et al.,2013**)¹³. Various

drug delivery nanosystems have been developed for overcoming GEM associated limitations. Among which encapsulation of GEM in nanocarrier turns out to be the best possible approach overcoming these obstacles, and can be utilized for safe and effective delivery of GEM. For instance, Aggrawal *et al.* developed GEM loaded polymeric nanoparticles (PLGA-b-PEG-NH₂ NPs) using water-in-oil-in-water (w/o/w) double emulsification method. It exhibited significant cytotoxic effect against pancreatic cancer cell lines (Aggrawal *et al.*, 2013)¹⁴. Similarly, enhanced efficiency of the drug delivery systems are required for the active targeting of GEM at the tumor site with minimal side effects.

In this study, gemcitabine-loaded galactosylated bovine serum albumin nanoparticles (GEM-LA-BSA NPs) were synthesized as an ASGPR-targeted nanocarrier for the effective treatment of HCC (as shown in **Figure 1**). The prime focus of this study is to improve the restorative efficacy of GEM by designing a ligand-targeted nanocarrier using lactobionic acid (LA), which is a biodegradable and biocompatible polysaccharide. Furthermore, it was cross-linked with BSA using amidation reaction to develop a network like structure to entrap hydrophilic therapeutic agents such as GEM. Recent studies have shown that the galactosylated BSA can be utilized as an ASGPR-targeting ligand, resulting in enhanced retention and permeability of NPs (Ahmed *et al.*, 2015; Li *et al.*, 2013)^{15,16}. Therefore, the conjugation of LA-BSA may lead to a site-specific delivery of GEM to tumorous cells. The conjugated nanoparticles were further optimized for best nanoformulation using central composite design in Design Expert 13.0 (Trial version 13.0, Stat-Ease Inc., Minneapolis, MN, USA). The conjugate:drug ratio was optimized for the formulation of nanoparticles and different response variables were observed like average particle size, zeta potential (Z.P), polydispersity index (PDI), drug loading (%), and entrapment efficiency (%). The optimized nanoparticles were further scrutinized for *in-vitro* drug release study for the ascertainment of release rate of GEM. Moreover, the morphological evaluation of the prepared nanoformulations was performed *via* high resolution transmission electron microscopy (HR-TEM). Furthermore, comparative *in-vitro* studies on HepG2 cell lines, and *in-vivo* studies in rat model were performed to estimate cell viability, cellular uptake, and pharmacokinetic profile of GEM-LA-BSA NPs, LA-BSA NPs, and free drug (GEM). Thus, the study hypothesized to exhibit the potential of the NPs to target liver cancer with improved pharmacokinetics of gemcitabine.

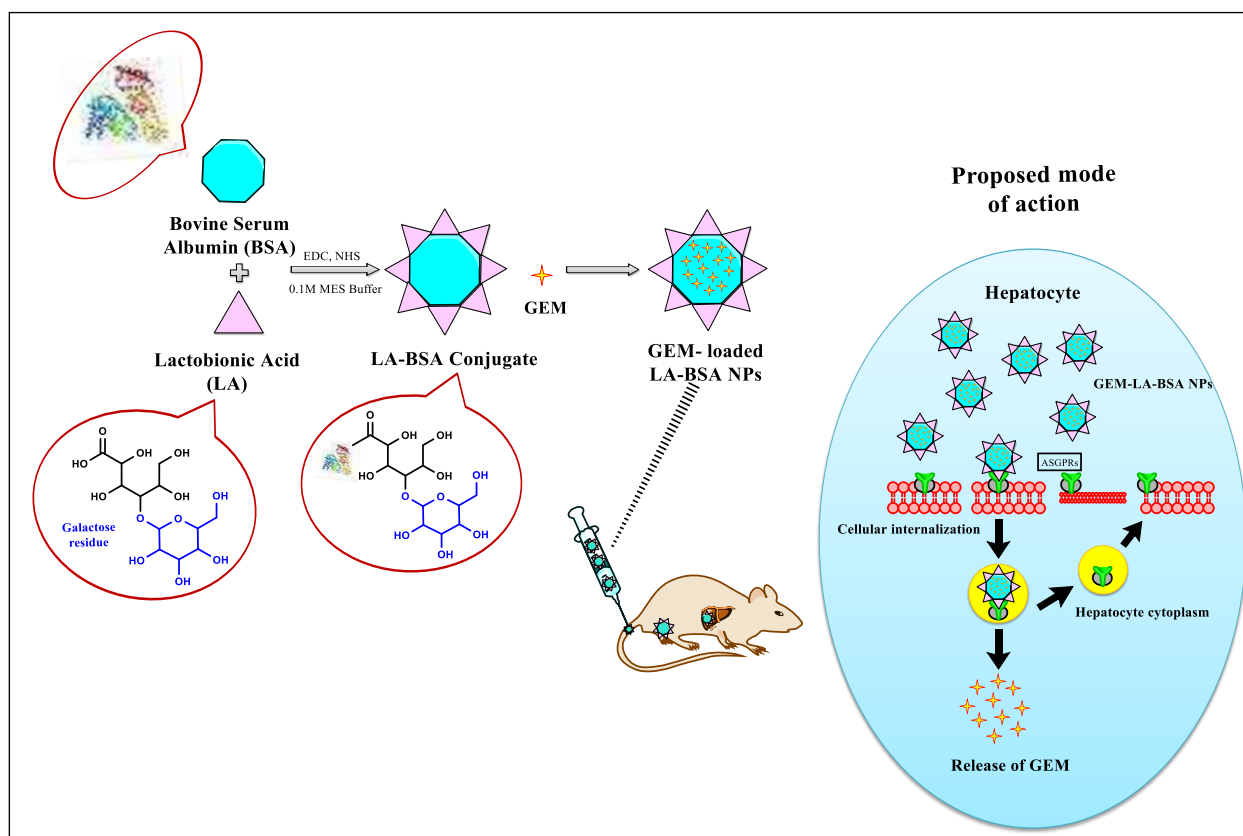


Figure 1: Graphical representation of the proposed study.

3. OBJECTIVES

- The primary objective of our study is to contrive a conjugate between LA and BSA for the active targeting to HCC cells.
- To develop a nanoparticulate-based formulation using galactosylation approach.
- To improve pharmacokinetic profile of GEM utilizing novel drug delivery system.
- To improve targetability of therapeutic moieties through galactosylation approach enabling a new platform of commercialization in-future.

4. MATERIALS AND METHODS

4.1 Materials

All the chemicals, reagents, and solvents used in this study were of analytical grade or above and were purchased from commercial suppliers. A gift sample of Gemcitabine HCl was received from Sun Pharmaceutical Industries Ltd., Vadodara, India. Bovine serum albumin Fraction V (BSA, purity 96–99%), glutaraldehyde for synthesis, glacial acetic acid, MES (2-(Morpholino)-

ethanesulfonic acid), and n-octanol were purchased from Molychem Ltd., New Delhi. Lactobionic acid (4-O-d-galactopyranosyl-d-gluconic acid, LA) was obtained from Sigma-Aldrich, USA. NHS (N-hydroxysuccinimide), EDC (N-(3-dimethylaminopropyl)-N-ethyl carbodiimide hydrochloride), and SAT (Sodium acetate trihydrate) were purchased from TCI Chemicals India. Acetonitrile and methanol were obtained of high performance liquid chromatography (HPLC) grade while ethanol and other reagents (acetone, DCM, etc.) were of analytical grade. All the reagents used in the study were purchased from Central Drug House (CDH), New Delhi. Dulbecco's Modified Eagle Medium (DMEM), 10% fetal bovine serum (FBS), and streptomycin and penicillin (SP) were purchased from Hi-Media (Carlsbad, CA, USA). HepG2, hepatocellular carcinoma cell line was purchased from National Center for Cell Science (NCCS), Pune. After receiving cell lines, the cells were transferred to perforated flasks and grown. Further, the flask was sub-cultured and stored under liquid nitrogen vapor for future use. All the experiments related to cells in this study were performed before 60 passages.

4.2 Synthesis and Characterization of LA-BSA Conjugates

Lactobionic acid (LA) (500 mg) was chemically conjugated to bovine serum albumin (BSA) using carbodiimide cross-linking chemistry (**Figure 2**). The synthesis of LA-BSA conjugate was based on the stoichiometric molar concentrations. Initially, LA (500 mg) was weighed and dissolved in de-ionized water. To this, 1mL of activating buffer solution i.e., 0.1M MES buffer (pH 5.5) was poured and mixed well. EDC (2.79 mmol, 534.84 mg) was added to this activated LA solution and subsequently after 15 min., NHS (1.5 mmol, 160.55 mg) was added with pH adjusted in between 5.0 - 6.0. The carbodiimide reaction mixture was kept on an ice-bath to maintain the temperature of the reaction and stirred over a magnetic stirrer for 2 h. This activated carboxyl groups and formed an unstable intermediate of amine reactive NHS ester. After 2 h, BSA (166.7 mg, 2 mL de-ionized water) was adjoined to the mixture with continuous stirring over an ice-bath for 24 h. After 24 h, the reaction was purified by membrane dialysis method followed by lyophilization. The solution was dialyzed using dialysis membrane-150 (Hi-Media, USA) (with 15,000 Da molecular weight cutoff) for 72 h in 100 mL of de-ionized water at RT. After purification, the LA-BSA conjugate was stored at -4 °C for further use. The synthesized LA-BSA conjugate was characterized by TLC, FT-IR, and ¹H-NMR spectroscopy (yield: 74%) (**Figure 2**) (Li et al., 2013; Thao et al., 2017)^{16,17}.

$$\% \text{ Yield} = \frac{\text{Practical Yield}}{\text{Theoretical Yield}} \times 100$$

-Eq.1

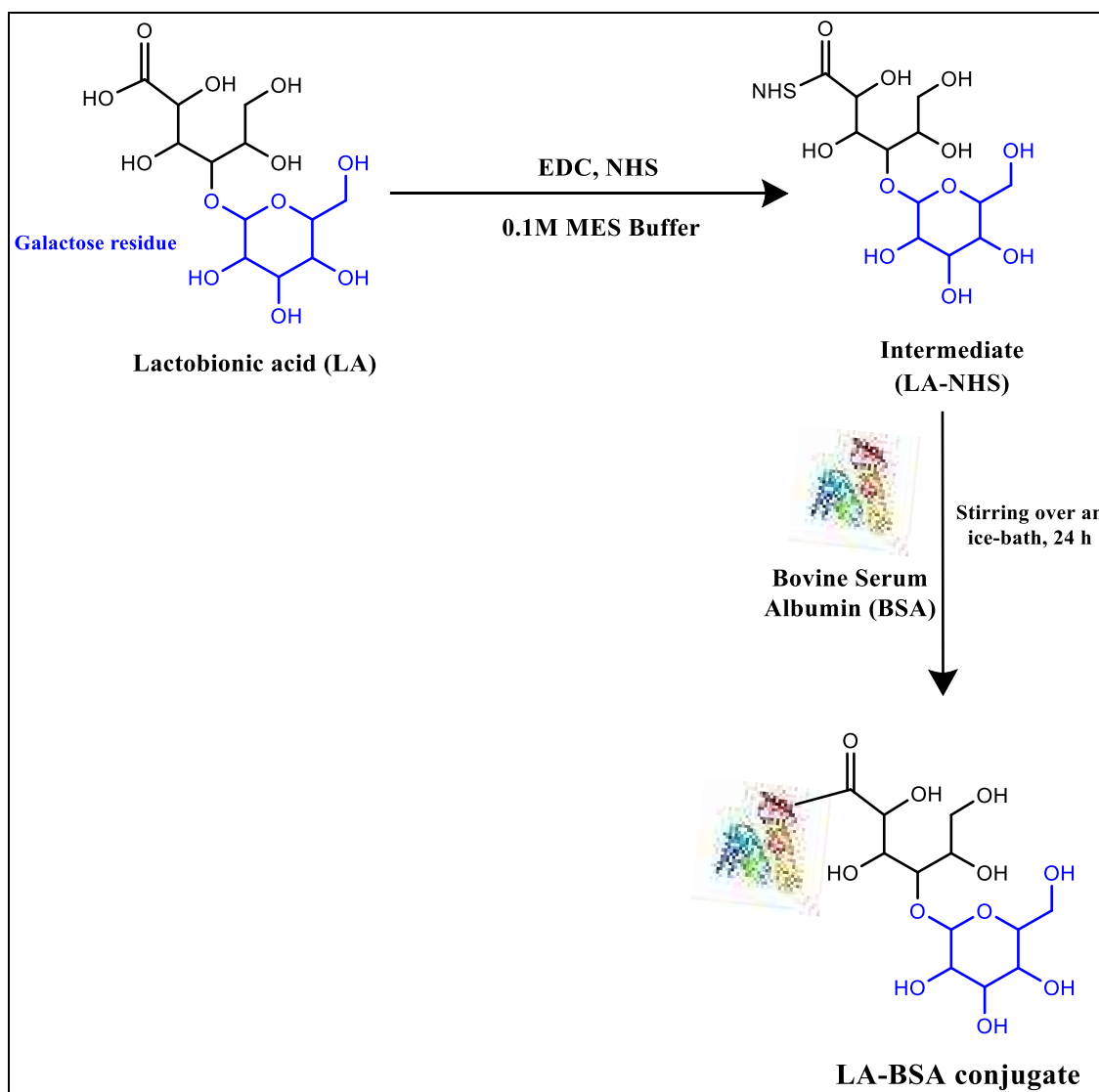


Figure 2: Synthetic representation of LA-BSA conjugates.

A TLC plate of dimension 4x 2 cm² was taken and 1 cm from the edge of the bottom a line was drawn called as base line. The spots were marked on the baseline with their specific codes, (G) represents drug solution (GEM), (L) represents lactobionic acid solution, (P) represents the product (LA-BSA conjugate) solution, and final spot (CO) represents the mobility of combination of all three spots. Then, the sample solutions were loaded on their respective

spots, and once loaded, they were kept in the mobile phase. Further, 20% DCM:MeOH was used as a mobile phase providing optimum results. Finally, the sample-loaded TLC plate was dried and analyzed under the U.V. cabinet (Model-1179, Jain Scientific Glass Works, India).

The synthesized LA-BSA conjugates (5 mg) were dissolved in 1 mL of deuterium based dimethyl sulfoxide (d-DMSO) in a NMR tube and sonicated for 8-10 min. at 25 °C. The LA-BSA conjugates were ascertained by ¹H-NMR spectroscopy using TopSpin software (Bruker Ascend-500 MHz, Switzerland) (Dayani et al., 2022)¹⁸.

The FT-IR spectroscopy was additionally performed to deduce and analyze the different functional groups of the synthesized conjugates. The changes in the conjugate structure were also confirmed by the FT-IR spectroscopy. The synthesized LA-BSA conjugate was mixed with potassium bromide (KBr) salt and triturated well using pestle-mortar. The interferogram was ascertained in the transmittance region of 4000 - 400 cm⁻¹ by FT-IR spectroscopy using Perkin Elmer software (Perkin Elmer, Spectrum Two, U.S.).

4.3 Design, Optimization and Preparation of Gemcitabine Loaded LA-BSA Nanoparticles (GEM-LA-BSA NPs)

GEM loaded LA-BSA NPs were prepared using the desolvation method with slight modifications. In this method, the NPs were fabricated by encapsulating GEM (mg) in the core of LA-BSA conjugate (2 % w/v, 40 mg). The concentrations of GEM and LA-BSA conjugates were optimized by Design-Expert version 13.0 (Trial version 13.0, Stat-Ease Inc., Minneapolis, MN, USA). The GEM loaded NPs (GEM-LA-BSA NPs) were obtained in different sizes with varied morphology. The design optimization of the GEM loaded NPs (GEM-LA-BSA NPs) were carried out using Central Composite Design.

4.3.1 Central Composite Design (CCD)

The preliminary step in preparing a formulation is optimization. The optimization of NPs can be performed by different methods; manual or software-based. In this study, the optimization of GEM-LA-BSA NPs was performed using a software-based method, i.e., central composite design (CCD) in Design Expert[®] software (Trial version 13.0, Stat-Ease Inc., Minneapolis, MN, USA) (Yalcin et al., 2018)¹⁹. The effect of weight of GEM (X1), and weight of LA-BSA conjugate (X2) on mean particle size (Y1), zeta potential (Y2), polydispersity index (Y3), drug loading (Y4), and encapsulation efficiency (Y5) were optimized using a two-factor, three-level

CCD. Each factor includes a set of three levels; where +1 and -1 are factorial points, $+\alpha$ and $-\alpha$ are axial points, and the centre point. These values were determined by reviewing available literature on polymeric NPs into consideration. The CCD was used with a total of 9 experiments comprising four factorial points, four axial points, and one center point. To maximize the drug loading (Y4), entrapment efficiency (Y5), and minimize the particle size (Y1) of NPs, the optimization of independent variables (X1 and X2) were investigated as shown in **Table 1**.

4.3.2 Preparation of GEM loaded LA-BSA NPs using desolvation method

Different concentrations of LA-BSA conjugate (w/v) and GEM were utilized to prepare and optimize the NPs. Initially, LA-BSA conjugate (0.25% w/v) and GEM (5 mg/mL) were dissolved in de-ionized water, separately. The LA-BSA conjugate solution was poured into a beaker and kept on magnetic stirrer at 400-500 rpm, RT. Further, GEM solution was added to the beaker in a drop-wise manner using a syringe, under continuous stirring. After 45 minutes, ethanol was also added drop-by-drop in the beaker under continuous stirring for another 1 h. After 1 h, 20 μ L of cross-linking agent, glutaraldehyde (1% v/v) was added with continuous stirring and kept on stirring overnight. The next morning, NPs formulated were centrifuged at 12,000 rpm for 30 minutes. The pellet obtained was re-dispersed in the supernatant in a fraction of seconds. Hence, 0.5 mL supernatant was pipetted out and made up to 2 mL with de-ionized water (**Figure 3**). The NPs sample was then analyzed using a UV-Visible spectrophotometer (Cary series-60, Agilent technology, Santa Clara, California) at 268 nm. The prepared nanoformulation was stored at -4°C for further characterization(**Weber et al., 2000**)²⁰.

Similarly, BSA NPs, LA-BSA NPs, and GEM-BSA NPs were also formulated and stored at -4°C for further characterization. The best formulation out of the CCD output was selected for further studies.

4.4 HPLC

Reverse phase high pressure liquid chromatography (RP-HPLC) was utilized to quantify the concentration of GEM in the prepared formulations (Shimadzu LC-2010 CHT, Tokyo, Japan).Merck HPLC column (RP C₁₈, 4.6 mm \times 250 mm), deuterium and tungsten lamp, and PDA detector was used in the chromatographic analysis. LC-Solution software was used for the data acquisition. The mobile phase utilized was acetonitrile (ACN): distilled water = 10:90 (%)

w/v), maintaining flow rate at 0.5 mL/min. and temperature at 25 ± 1 °C. The injection volume was kept constant at 20 µL and aliquots ranging from 0.1 to 5 µg/mL for the preparation of calibration curve *via* HPLC method. The detection wavelength (λ_{max}) of GEM was 268 nm and the retention time was observed to be 9.5 min (Khare et al., 2016)²¹.

4.5 Characterization of GEM loaded LA-BSA NPs

4.5.1 Morphology (by HR-TEM)

The shape and surface related morphological characteristics of BSA NPs, LA-BSA NPs, GEM-BSA NPs, and GEM-LA-BSA NPs were delineated by high resolution transmission electron microscopy (HR-TEM) (Cryo-TEM Talos S, Thermo Scientific, US) in SAIF-AIIMS, New Delhi. The TEM samples were prepared by drop-on-grid method, the samples stowed on a copper grid followed by the insertion of grid in the equipment and the photomicrographs were observed.

4.5.2 Particle Size, Zeta Potential and Polydispersity Index

The particle size and size distribution of different batches of GEM-LA-BSA NPs, GEM-BSA NPs, LA-BSA NPs, and BSA NPs were determined through nanozetasizer (Malvern, UK) where samples were diluted 10 times with the de-ionized water. The final size measurements were characterized by dynamic light scattering at a specific angle and temperature, 90° and 25 °C, respectively. The report was generated from Zetasizer version 711.

4.5.3 Percentage Drug Loading (DL) and Entrapment Efficiency (EE)

The GEM-LA-BSA NPs were characterized using the percentage of a drug (GEM) encapsulated in the formulation. Encapsulation was determined using the membrane dialysis method. A specified volume of sample was withdrawn from each formulation and introduced in the separate dialysis membrane (MWCO 5 kDa, Hi-Media Laboratories Pvt. Ltd., India). Then, the dialysis membrane was immersed in a beaker containing 50 mL de-ionized water kept over a magnetic stirrer. At the predetermined intervals, 0.5 mL aliquots were withdrawn from the sink with replacement maintaining absolute sink conditions. Finally, the aliquots withdrawn were analyzed using a UV-Visible spectrophotometer (Cary series-60, Agilent technology, Santa Clara, California) (Nair et al., 2019)²². The withdrawn samples were also analyzed by RP-HPLC

(Shimadzu LC-2010 CHT, Tokyo, Japan) using acetonitrile (ACN): distilled water = 10:90 (% w/v) as the mobile phase with 0.5 mL/min flow rate at 268 nm (Khare et al., 2016)²¹. Mathematically, the percentage drug loading (%DL) and entrapment efficiency (%EE) can be calculated as:

$$\% DL = \frac{\text{Weight of total theoretical drug} - \text{Weight of unentrapped drug}}{\text{Weight of total carrier}} \times 100$$

-Eq. 2

$$\% EE = \frac{\text{Weight of total theoretical drug} - \text{Weight of unentrapped drug}}{\text{Weight of total drug taken}} \times 100$$

-Eq. 3

4.5.4 *In-vitro* Drug Release

In-vitro release profile of GEM from GEM-LA-BSA NPs were estimated against pure drug (GEM) and GEM-BSA NPs in PBS (pH 7.4) using the membrane dialysis method. Briefly, 1mL of prepared formulations and pure drug was taken in a separate dialysis membrane (MWCO 5 kDa, Hi-Media Laboratories Pvt. Ltd., India), tied from both the ends and immersed in 100 mL of PBS buffer (pH 7.4) in separate beakers, kept over a magnetic stirrer at 500-600 rpm for 24 h, at 37 ± 2 °C. 1mL aliquots were extracted at predetermined time intervals with replacements from all the beakers and replenished with the same amount of buffer to sustain sink conditions. Then, the samples were ascertained using UV-visible spectrophotometer (Cary series-60, Agilent technology, Santa Clara, California) and RP-HPLC (Shimadzu LC-2010 CHT, Tokyo, Japan) using acetonitrile (ACN): distilled water = 10:90 (% w/v) as the mobile phase at 268 nm. Moreover, cumulative percent drug release (% DR) was depicted and plotted against time (Dora et al., 2017)²³. The release study was carried out in triplicate.

4.5.5 Stability Studies

Time and temperature dependent stability studies were carried out for different NPs upto 180 days. All the developed formulations i.e. BSA NPs, LA-BSA NPs, GEM-BSA NPs, and GEM-LA-BSA NPs were stored at different temperatures (4, 25, and 45 °C), over a span of 6 months. After 6 months, all the developed formulations were diluted 10 times with de-ionized water, filtered and evaluated for particle size distribution for determining the stability of developed NPs. The formulations were also observed for any physical change such as color change, precipitation, turbidity or any other observable change.

4.5.6 Hemolytic Studies

The concentration-dependent hemolytic effect of BSA NPs, LA-BSA NPs, GEM-BSA NPs, and GEM-LA-BSA NPs was carried out with erythrocytes (RBCs) suspension, in accordance with an established procedure (**Slowing et al., 2009**)²⁴. The human blood sample was collected from a healthy volunteer in tube having EDTA. Further, it was centrifuged (R-4C DX, REMI, India) to separate the serum from the erythrocytes at 2000 rpm for 10 min. The collected erythrocytes were washed thrice using normal saline (0.9% w/v NaCl) and diluted upto 10 times with 0.9% w/v NaCl solution. The erythrocytes suspension (80 µL) was mixed with 2, 5, and 10 µL of developed formulations to prepare the final concentration 20, 50, and 100 µg/mL. It was assumed that erythrocytes in de-ionized water exhibits complete hemolysis (100% control value) thus it was regarded as a positive control whereas, in normal saline as a negative control. The erythrocytes suspensions were incubated for 1 h and further centrifuged at 1500 rpm for 2-5 min. The supernatant was ascertained at 540 nm using UV–visible spectrophotometer (Cary series-60, Agilent technology, Santa Clara, California). The results were performed in triplicate. Mathematically, the percentage hemolysis was calculated using the following formula.

$$\% \text{ Hemolysis} = \frac{\text{Absorbance of test} - \text{Absorbance of negative control}}{\text{Absorbance of positive control} - \text{Absorbance of negative control}} \times 100$$

-Eq. 4

4.5.7 Cytotoxicity by MTT assay

The cytotoxic behavior of GEM-LA-BSA NPs against pure drug (GEM), GEM-BSA NPs, and LA-BSA NPs was investigated in HepG2 cell lines through MTT assay (**Tekchandani et al., 2020, Mosmann, 1983**)^{25,26}. HepG2 cells were grown and cultured in the perforated flask using Dulbecco's Modified Eagle Medium (DMEM) with 10% purified fetal bovine serum (FBS) and 1% antibiotic (penicillin-streptomycin). The confluent flask (upto 85% cell growth) was trypsinized to detach the adhered cells and centrifuged for 5-6 min at 1000-1500 rpm. The obtained cells pellet was re-dispersed in 2 mL of freshly prepared culture media. A small quantity of re-dispersed suspension with equivalent quantity of trypan blue dye was utilized for the determination of percent cell viability using hemocytometer and the specific concentration to be used was determined (Marienfield, Germany).

The cells were seeded in 96-well plates, maintaining the cell concentration to be 5×10^3 cells per well. The seeded plates were incubated in a CO₂ incubator (Thermo-Fisher Heracell 150i) for

24 h. Different concentrations (10 to 800 µg/mL) of samples were prepared in the culture media. The media seeded in 96-well plates was removed thoroughly for the treatment of plates with the mentioned formulations of different concentrations, followed by incubation for 24 h. After 24 h, the treated plates were thoroughly washed with PBS (pH 7.4). After PBS washing, 50 µL of MTT solution (5% in water) was added into each well and incubated for 4 h. After 4 h, the formazan crystals were developed which were dissolved by the addition of 150 µL DMSO to each well. Finally, the plates were analyzed for absorbance values using a Microplate reader (Omega Fluster, BMG Labtech) at 570 nm. The IC₅₀ values of each formulation were calculated using GraphPad Prism 8.0 software. All the cytotoxicity studies were carried out at least three times.

4.5.8 Cellular Internalization Studies

The qualitative and quantitative cellular uptake studies of pure drug and drug-loaded formulations (GEM, GEM-BSA NPs, LA-BSA NPs, and GEM-LA-BSA NPs) were carried out in HepG2 cell lines. Briefly, 6-well plates were seeded with the HepG2 cells uniformly with cell concentration of 5×10^3 cells per well, followed by overnight incubation. The developed formulations were tagged with freshly prepared fluorescein isothiocyanate (FITC) solution to evaluate cellular uptake.

Firstly, 5 µL of developed formulations were dissolved in 1 mL of PBS (pH 7.4) in the separate vials. Further, 5 mg FITC was dissolved in 2 mL of fresh acetone. Among which, 0.4 mL freshly prepared FITC solution was added to the previously prepared solutions and kept on stirring for 12-16 h. After 12-16 h, the untagged FITC was removed by the dialysis membrane method against PBS (pH 7.4). Further, 1.2 mL of freshly prepared DMEM media was added to the FITC tagged reaction and mixed well.

Secondly, the cells seeded in 6-well plates were washed using PBS (pH 7.4) before the treatment of FITC-tagged formulations. The DMEM media was removed from the wells, followed by PBS washing after 2, 4 and 6 h. Pure FITC was considered as a control. Fluorescence microscopy was performed to evaluate the extent of cellular internalization using a fluorescent microscope (Olympus CKXF3, Japan). The fluorescence intensity was determined quantitatively using ImageJ software (National Institutes of Health, University of Wisconsin, USA). All the cell line based studies were carried out at least three times.

4.5.9 *In-vivo* Pharmacokinetic Studies

In-vivo pharmacokinetic studies were carried out in Rungta College of Pharmaceutical Sciences and Research in accordance following ethical guidelines. The permission was obtained from the Institutional Animal Ethic Committee (IAEC) under the reference number RCPSR/IAEC/2022/28. Sprague Dawley (SD) rats (7–8 weeks old, 200–250 g, n = 4) were utilized for the determination of pharmacokinetic profile of the GEM-LA-BSA NPs against free drug (GEM). The SD rats were contingently splitted into 3 groups with 4ratsper group among which negative group was treated with normal saline (0.9% w/v NaCl) and the positive groups were treated with the control (GEM) and developed formulations (GEM-BSA NPs and GEM-LA-BSA NPs (1 mg/kg of body weight, thrice per week)).The SD rats were kept on fasting overnight before experiment for significant results. All the rats were administrated *via* intravenous route (*via* tail vein) for 14 days. A single dose of 1 mg/kg (equivalent to pure drug) of the formulations and pure drug was given to the animals (except normal control group) and 0.2 mL of blood sample was collected from the retro-orbital plexus in heparinized tubes with heparin at specific intervals 0.5, 1, 2, 4, 8, 16, 24 and 48 h after anesthetizing animals by chloroform. Plasma was isolated by centrifugation at 4000-5000 rpm for 20 min at 4°C. Finally, estimation of drug content will be done by RP-HPLC method using acetonitrile (ACN): distilled water = 10:90 (% w/v) as the mobile phase at 268 nm (Paul et al., 2019)²⁷.

5. Results

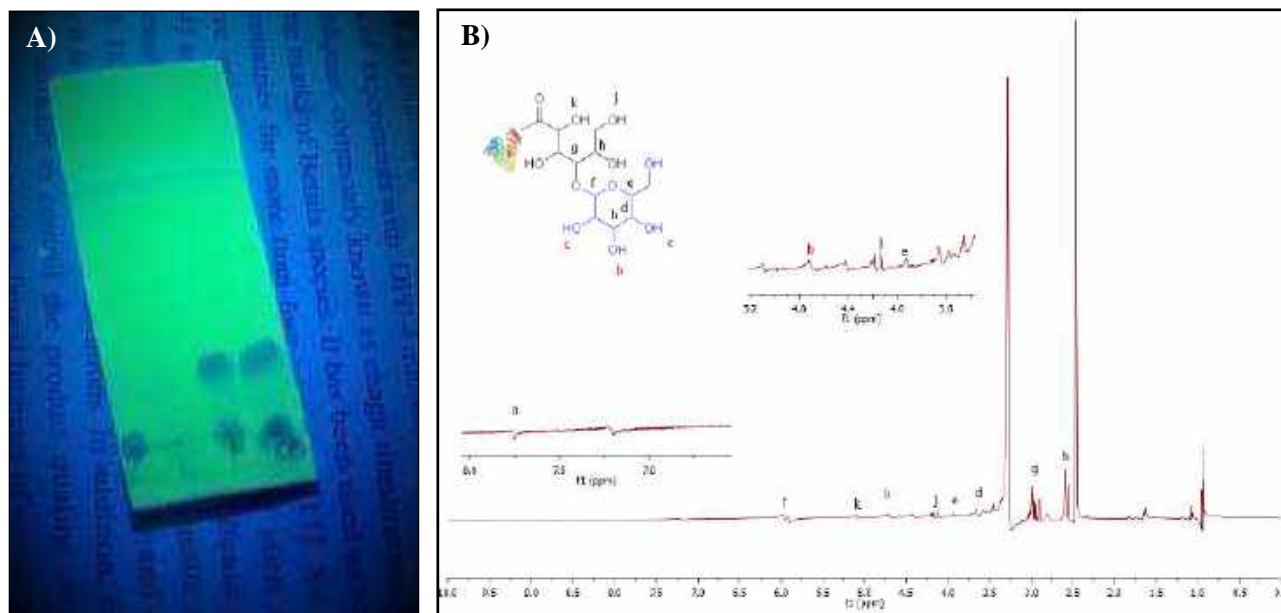
5.1 Characterization of LA-BSA Conjugate

The carboxylic acid of lactobionic acid forms an amide linkage with BSA which leads to the formation of the LA-BSA conjugate. It was characterized by TLC using 20% DCM:MeOH as a mobile phase as shown in **Figure 3A**.In TLC, an equal level of mobility was observed between spot (P) and spot (CO) which indicates the completion of LA-BSA conjugate synthesis. In addition, it was confirmed by ¹H–NMR spectroscopy (Bruker Ascend-500.3 MHz, Switzerland) using d-DMSO as the solvent.

In **Figure 3B**,¹H-NMR (500 MHz, d-DMSO) δ ppm: 7.75 [-CONH (a)], 4.75 [OH (b)], 3.85 [OH (c)], 3.65 [-CH (d)], 3.9 [-CH (e)], 5.56 [CH (f) chemical peak shifted due to the presence of neighboring electronegative atoms], 3.0 [-CH (g)], 2.65 [-CH (h)], 4.15 [OH (j)], 5.15 [OH (k)], of lactobionic acid conjugated with BSA (Pavia et al., 2001)²⁸. Chemical shift of COOH group

present in the BSA did not appear as the group was bound with LA to form amide linkage. The absence of free -COOH group in the NMR spectrum confirmed the reaction completion and synthesis of LA-BSA conjugate (Dayani et al., 2022)¹⁸.

In **Figure 3C**, FT-IR spectra of LA, BSA, and LA-BSA conjugates were showcased. In the interferogram of LA (a), the characteristic peaks were observed at 3396.7, 2926.4, 1740.4 and 1073.7 cm^{-1} , attributing to the stretching bands of -OH, H-C, -C=O (-COOH), and heterocyclic C-O-C, respectively. While, the interferogram of BSA (b) exhibits the characteristic peaks at 3376.3, 1654.5 and 1548.1 cm^{-1} attributing to the stretching bands of N-H, -C=O (amide), and bending bands of N-H (amide), respectively. However, the interferogram of LA-BSA conjugate (c) exhibits the characteristic bands of amide linkage with increased intensity at 1636.4 and 1709.2 cm^{-1} , attributing to the stretching bands of acetyl group (-C=O, amide) and bending bands of N-H ($\text{O}=\text{C}-\text{NH}_2$, amide), respectively. Meanwhile, the characteristic carbonyl (-C=O) peak of LA at 1740.4 cm^{-1} was vanished in the conjugated curve indirectly confirming the formation of LA-BSA conjugate *via* amidation reaction. The absence of additional peaks of LA or BSA in the LA-BSA curve also confirms the conjugate formation.



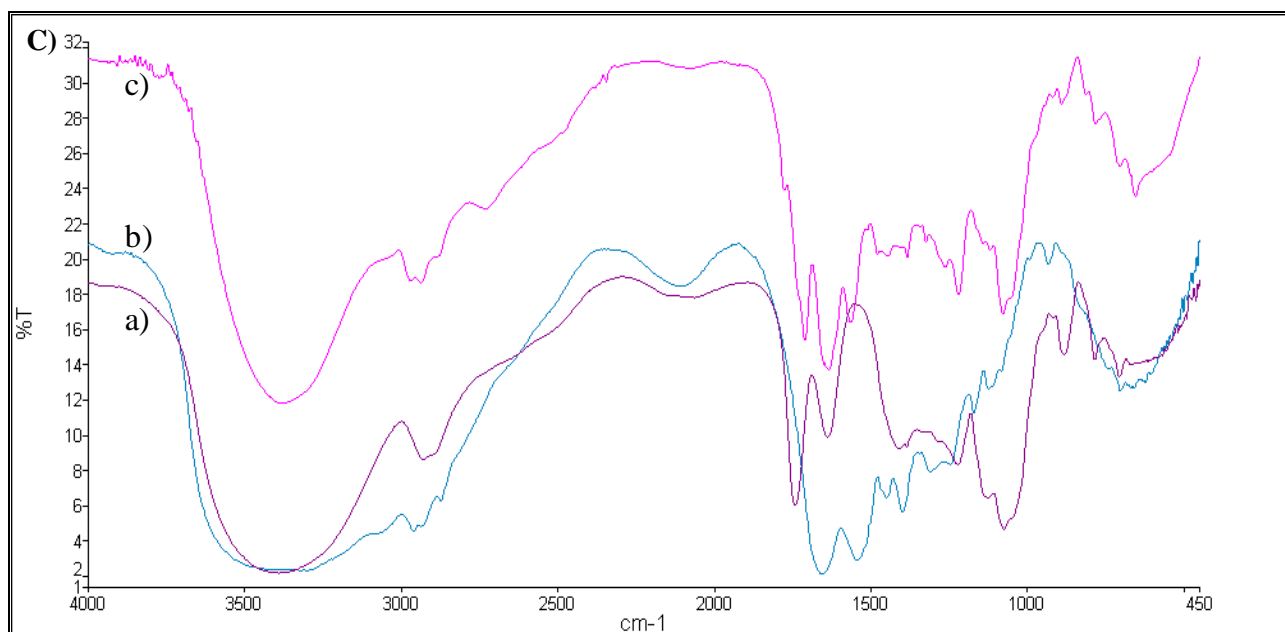


Figure 3: A)TLC of LA-BSA conjugate using 20% DCM: MeOH as a mobile phase, B) ^1H -NMR spectrum of the LA-BSA conjugate. DCM- Dichloromethane; MeOH- Methanol, and C) FT-IR spectra of a) lactobionic acid (LA), b) bovine serum albumin (BSA), and c) lactobionic acid-bovine serum albumin conjugate (LA-BSA conjugate).

5.2 Optimization of Galactosylated Albumin-based Nanoparticles

Galactosylated albumin-based nanoparticles (GEM-LA-BSA NPs) were prepared by the modified desolvation method (Li et al., 2013)¹⁶.

5.2.1 Central Composite Design (CCD)

The optimization of the formulation was carried out by the Central Composite Design in the Design Expert 13.0 software.

Table 1: Optimization of different batches of GEM-LA-BSA NPs using Central Composite Design.

	Std	Run	Factor 1 A:GEM mg	Factor 2 B:LA-BSA conjuga... %	Response 1 P.S nm	Response 2 Z.P mV	Response 3 PDI -	Response 4 DL %	Response 5 EE %
	4	1	12.5	5	181.47	-0.22	0.505	3.6	29.88
	8	2	8.75	5.62	204.83	-0.15	0.515	2.09	27.45
	5	3	3.45	3.5	130.2	0.23	0.369	2.44	35.78
	3	4	5	5	220	0.3	0.5	2.8	45.5
	7	5	8.75	1.38	171.55	-0.21	0.5	10.08	47.2
	6	6	14.05	3.5	211.4	0.88	0.637	9.76	53.89
	2	7	12.5	2	228.65	0.33	0.64	12.16	73.81
	9	8	8.75	3.5	221.55	18.7	0.468	4.94	39.52
	1	9	5	2	115	0.25	0.242	2.68	13.7

Table 2: Depicts regression analysis for measured responses- GEM-LA-BSA NPs.

Summary of results of regression analysis for measured responses					
Parameters	P.S	Z.P	PDI	DL	EE
Model	2-FI	Quadratic	2-FI	2-FI	2-FI
R ²	0.8578	0.9991	0.9671	0.9776	0.9437
Adjusted R ²	0.7725	0.9976	0.9474	0.9642	0.9100
Predicted R ²	0.7210	0.9930	0.8706	0.9195	0.7968
SD	19.67	0.3021	0.0283	0.7439	5.18
% CV	10.51	13.52	5.82	13.25	12.71
SS	5789.69	305.55	0.0386	18.84	1433.76
DF	1	2	1	1	1
F-Value	14.96	1674.34	48.23	34.03	53.48
P-Value	0.0118	<0.0001	0.0010	0.0021	0.0007
Significance	Significant	Significant	Significant	Significant	Significant

5.2.1.1 Effect on Particle Size (P.S)

The particle size of formulations was recorded in the range of 115 to 230 nm, based on the different values of independent variables as well as dependent variables (**Table 1**). **Figure 4a & b** represents contour plot and 3D response surface plot, respectively which articulates the effect of independent variables (X1 and X2) on the particle size.

Mathematically, it can be represented as:

$$\text{Mean particle size (Y1)} = 30.00581X_1 + 67.92453X_2 - 6.76356X_1X_2 - 105.96945 \quad \text{-Eq. 5}$$

5.2.1.2 Effect on Zeta Potential

The zeta potential (Z.P) of formulations was recorded to be in the range of 19 to -0.22 mV. Lowest magnitude of Z.P (-0.22 mV) was observed for the formulation of batch 1, whereas, the highest Z.P (18.7 mV) was observed for the formulation of batch 8, as depicted in **Table 1**. The effect on Z.P was depicted by the quadratic model design which was effectively utilized for the determination of correlation coefficient. **Figure 4c & d** represents contour plot and 3D response

surface plot, respectively which articulates the effect of independent variables (X1 and X2) on the Z.P.

Mathematically, it can be represented as:

$$\text{Z.P (Y1)} = 11.41341X_1 + 29.60375X_2 - 0.026667X_1X_2 - 0.645949X_1^2 - 4.20072 X_2^2 - 83.04950 \quad \text{-Eq. 6}$$

5.2.1.3 Effect on Polydispersity Index

Polydispersity index (PDI) of formulations was recorded to be in the range of 0.24 to 0.64, based on the different values of independent variables as well as dependent variables. **Figure 4 e & f** represents contour plot and 3D response surface plot, respectively which articulates the effect of independent variables (X1 and X2) on the particle size.

Mathematically, it can be represented as:

$$\text{PDI (Y1)} = 0.087209X_1 + 0.164857X_2 - 0.017467X_1X_2 - 0.318938 \quad \text{-Eq. 7}$$

5.2.1.4 Effect on Drug Loading

Drug Loading (DL) was determined in de-ionized water, by a membrane dialysis method. It is based on the determination of the amount of the drug incorporated into a polymeric matrix. The calculated DL for different batches ranges between 2.09 to 12.16%. The effect of DL was depicted by 2-FI model design as mentioned in the **table 1**. **Figure 4g & h** represents contour plot and 3D response surface plot, respectively which articulates the effect of independent variables (X1 and X2) on the percent drug loading.

Mathematically, it can be represented as:

$$\text{DL (Y2)} = 2.03817X_1 + 1.73015X_2 - 0.385778X_1X_2 - 6.45842 \quad \text{-Eq. 8}$$

5.2.1.5 Effect on Entrapment Efficiency

Entrapment efficiency (EE) is a ubiquitous parameter can also be calculated using a membrane dialysis method. The calculated %EE ranged from 13.7% to 73.81%. The effect of CCD on entrapment efficiency was obtained to be significant using 2-FI model design as mentioned in **Table 2**. **Figure 4 i & j** represents contour plot and 3D response surface plot, respectively which articulates the effect of independent variables (X1 and X2) on the percent entrapment efficiency (EE).

Mathematically, it can be represented as:

$$EE (Y3) = 14.11786X1 + 26.11153X2 - 3.36578X1X2 - 71.09691$$

-Eq. 9

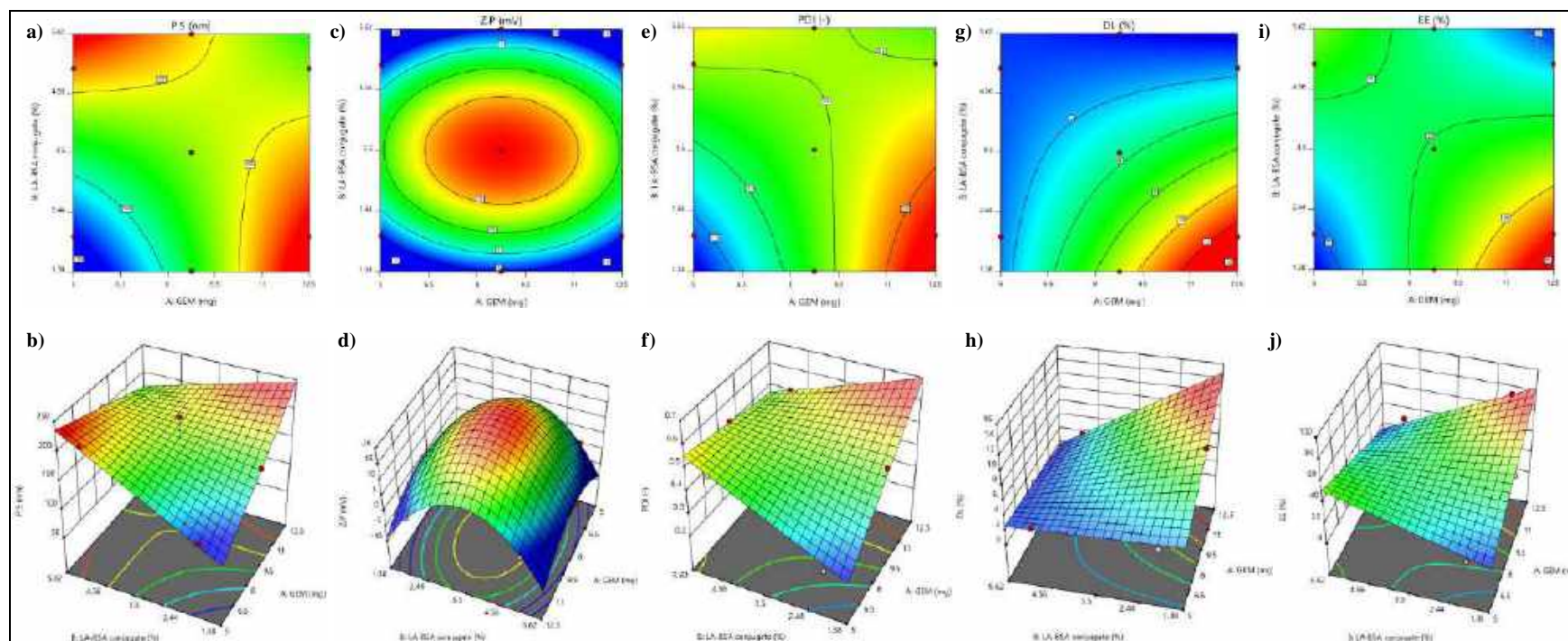


Figure 4: Graphical representation of the effects of particle size (a & b), zeta potential (c & d), polydispersity index (e & f), drug loading (g & h), and entrapment efficiency (i & j) on the preparation of GEM-LA-BSA NPs by central composite design (CCD) (n = 9).

5.3 Characterization of GEM-LA-BSA NPs

5.3.1 Morphological characteristics

The structural morphology of the prepared nanoformulations was observed under high resolution transmission electron microscopy (HR-TEM) and thereby photomicrographs were acquired. The BSA NPs and GEM-BSA NPs seem to be spherical in shape exhibiting a nanometric size range (**Figure 5**). Also, LA-BSA NPs seems to have a double layered spherical shaped morphology exhibiting highly negative charge. The outer crust reflects the presence of lactobionic acid (LA), while GEM-LA-BSA NPs were observed as agglomerate which illustrates the strong network of nanoparticles.

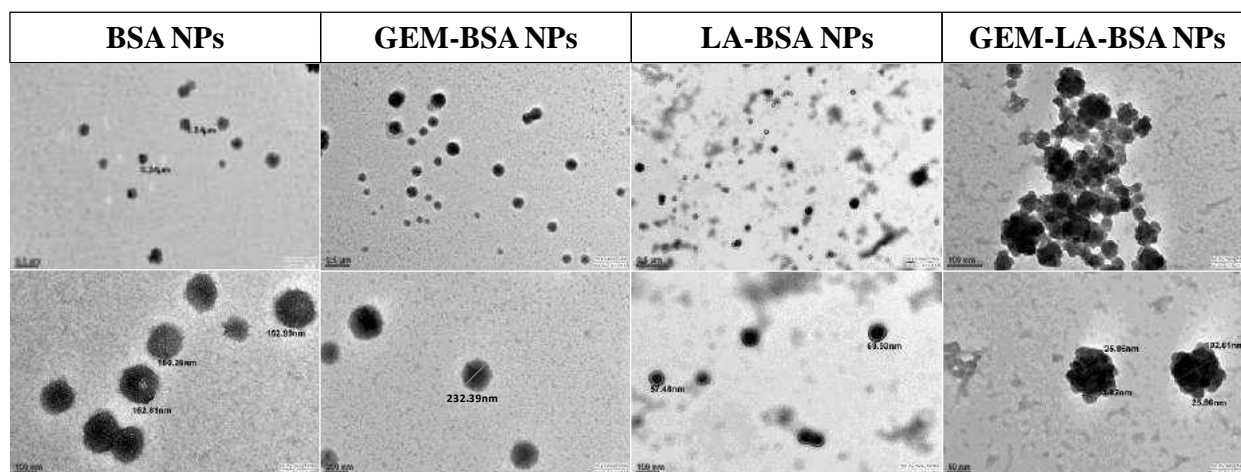


Figure 5: Morphological analysis of BSA NPs, GEM-BSA NPs, LA-BSA NPs, and GEM-LA-BSA NPs using high resolution transmission electron microscopy (HR-TEM). The two scales are 0.5 μm -100 nm and 50-200 nm.

5.3.2 Particle Size, Zeta Potential, and PDI

Table 3: Particle size, PDI, and zeta potential of the prepared formulations. Values represents mean \pm SD (n=3).

Formulation	Particle size (nm)	PDI	Zeta Potential (mV)
BSA NPs	355.4 \pm 28.43	0.3 \pm 2.43	0.2 \pm 0.1
LA-BSA NPs	97.59 \pm 9.67	0.27 \pm 0.016	4.1 \pm 0.8
GEM-BSA NPs	96.77 \pm 7.86	0.25 \pm 0.01	8.5 \pm 0.7
GEM-LA-BSA NPs	71.52 \pm 4.05	0.27 \pm 0.081	9.0 \pm 1.4

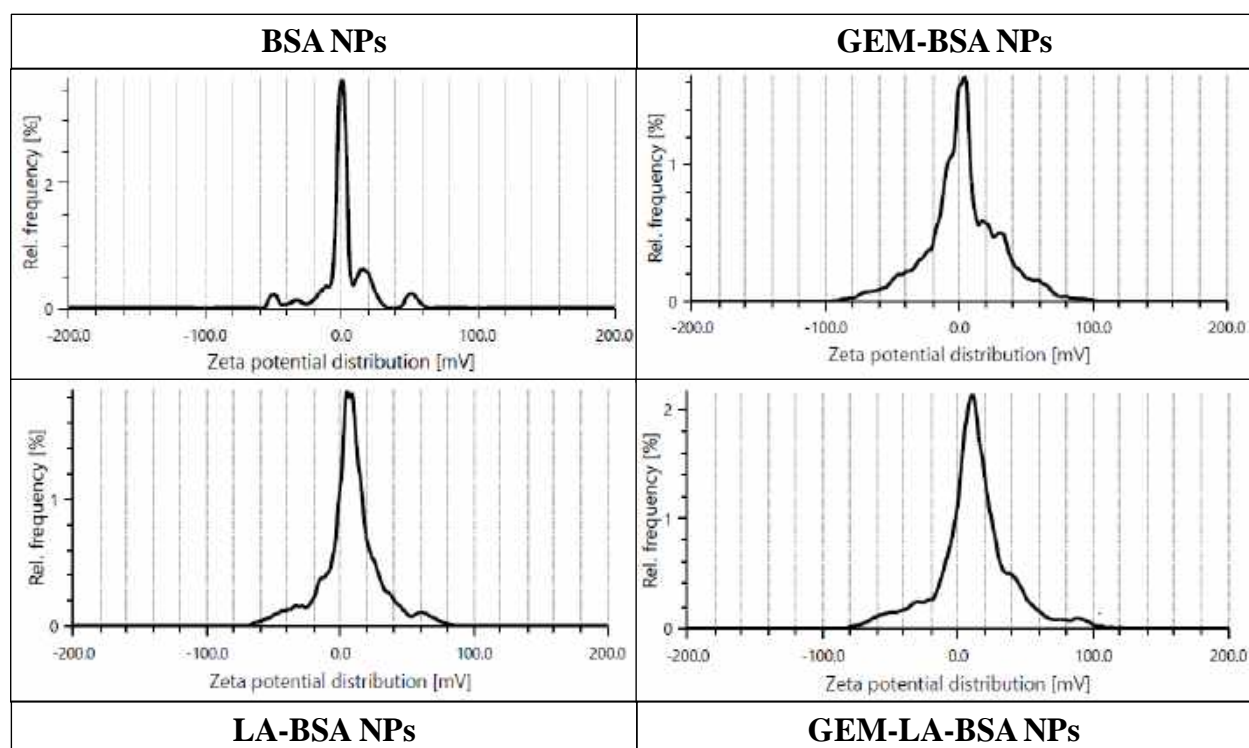


Figure 6: Zeta potential (mV) distribution of BSA NPs, LA-BSA NPs, GEM-BSA NPs, and GEM-LA-BSA NPs using Anton Paar Litesizer 500.

5.4 Percentage Drug Loading and Entrapment Efficiency

The clinical repercussions of GEM-LA-BSA NPs may be estimated by the percentage drug loading (%DL) and entrapment efficiency (%EE). The hydrophilicity of GEM was observed to be the cause of reduced drug loading and entrapment efficiency, i.e. $1.86 \pm 0.093\%$ and $15.19 \pm 0.68\%$ respectively. Further, different concentrations of GEM-LA-BSA NPs were prepared for characterization and it was analyzed using a UV-visible spectrophotometer (Cary series-60, Agilent technology, Santa Clara, California) and RP-HPLC (Shimadzu LC-2010 CHT, Tokyo, Japan) using acetonitrile (ACN): distilled water = 10:90 (% w/v) as the mobile phase at 268 nm (**Table 1**). Further, the results were compiled graphically using Design-Expert Version 13.0 (CCD) (**Figure 4**).

5.5 In-Vitro Drug Release

The membrane dialysis method was utilized for the determination of *in-vitro* drug release profile. A comparative study was performed on the GEM against the formulations prepared. It was

observed that the GEM-LA-BSA NPs exhibited 57.78 ± 4.10 % of drug release even after 48h, while GEM-BSA NPs and GEM exhibited $96.32 \pm 3.85.10\%$ and 99.23 ± 3.28 % of drug release at pH 7.4, respectively. Hence, it was determined that GEM-LA-BSA NPs are more efficacious than free drug (GEM) as it follows the sustained drug release pattern (**Figure 7**).

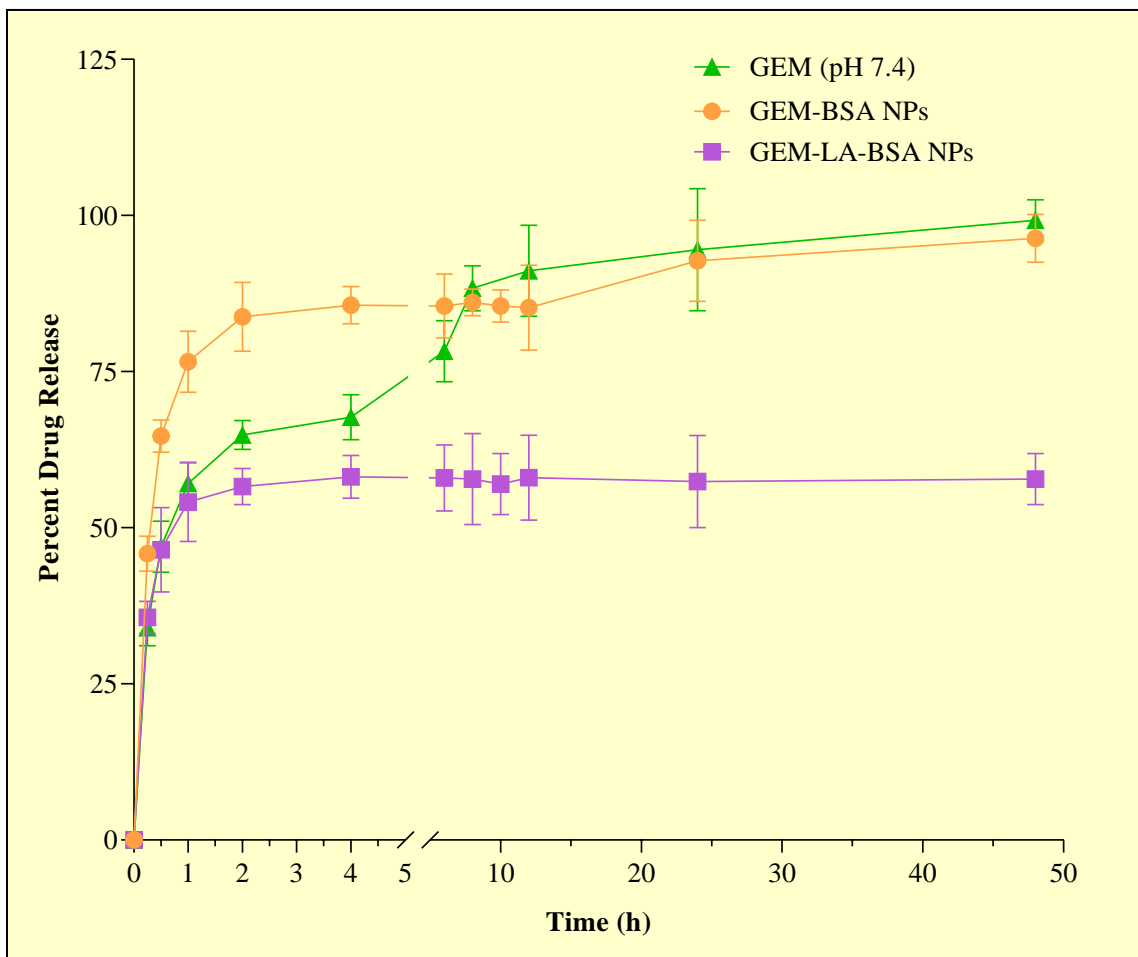


Figure 7: *In-vitro* drug release of GEM, GEM-BSA NPs, and GEM-LA-BSA NPs in phosphate buffer saline (PBS) pH 7.4 at 37 ± 2 °C. Values represents mean \pm SD (n=3).

5.6 Stability Studies

Physical stability of nanoparticles is associated with particle size and zeta potential of the dispersion. The storage stability studies conducted for optimized BSA NPs, LA-BSA NPs, GEM-BSA NPs, and GEM-LA-BSA NPs at 4, 25, and 45 °C for 6 months. After 6 months of storage, the particle size determination indicates a slight difference whereas there was no

significant difference in the zeta potential which indicates a desirable stability of the formulation (**Table 4**). The agglomerates formation of GEM-LA-BSA NPs tends to reduce the desired stability slightly. A significant color change, precipitation, and change in consistency was observed at 45 °C. At room temperature (25 °C), there was a slight change in color and consistency. However, the formulation was found to be stable in every aspect at 4 °C as depicted in **Table 4**. It may be due to the presence of albumin based nanocarriers which tends to be stable at cool temperature. Many research groups has established that the albumin based formulation are more stable in a cool temperature than room or warm temperature (**Wu et al.,2011; Jun et al., 2011**)^{29,30}.

Table 4: Physical changes observed after stability studies of BSA NPs, LA-BSA NPs, GEM-BSA NPs, and GEM-LA-BSA NPs at different temperatures (4, 25, and 45 °C). Values represents mean \pm SD (n=3).

Parameters	Formulations	Temperature		
		4 °C	25 °C	45 °C
Color change	LA-BSA NPs	-	-	++
	GEM-BSA NPs	-	+	++
	GEM-LA-BSA NPs	-	+	++
Precipitation	LA-BSA NPs	-	+	++
	GEM-BSA NPs	-	-	++
	GEM-LA-BSA NPs	-	-	++
Turbidity	LA-BSA NPs	+	++	-
	GEM-BSA NPs	-	-	++
	GEM-LA-BSA NPs	-	-	-
Crystallization	LA-BSA NPs	++	-	-
	GEM-BSA NPs	++	-	-
	GEM-LA-BSA NPs	++	-	-

Change in consistency/ volume	LA-BSA NPs	-	-	++
	GEM-BSA NPs	-	++	++
	GEM-LA-BSA NPs	-	++	++

(-) Indicate no change, (+) indicate slight change, and (++) indicate significant change.

Table 5: Stability studies of LA-BSA NPs, GEM-BSA NPs, and GEM-LA-BSA NPs at different temperatures (4, 25, and 45 °C). Values represents mean \pm SD (n=3).

Parameters	Formulations	Temperature		
		4 °C	25 °C	45 °C
Particle Size (nm)	LA-BSA NPs	626.07 \pm 219.5	469.90 \pm 148.2	338.80 \pm 110.4
	GEM-BSA NPs	167.30 \pm 3.6	161.10 \pm 13.5	412.63 \pm 105.0
	GEM-LA-BSA NPs	227.93 \pm 13.8	140.43 \pm 8.0	206.17 \pm 54.0
Zeta Potential (mV)	LA-BSA NPs	1.19 \pm 1.27	6.78 \pm 0.80	3.98 \pm 1.41
	GEM-BSA NPs	8.47 \pm 1.20	7.38 \pm 0.08	6.35 \pm 0.95
	GEM-LA-BSA NPs	15.37 \pm 3.48	13.33 \pm 2.18	8.83 \pm 1.60
Polydispersity Index	LA-BSA NPs	0.158 \pm 0.16	0.100 \pm 0.10	0.071 \pm 0.07
	GEM-BSA NPs	0.116 \pm 0.12	0.043 \pm 0.04	0.138 \pm 0.14
	GEM-LA-BSA NPs	0.147 \pm 0.15	0.019 \pm 0.02	0.156 \pm 0.16

5.7 Hemolytic Studies

The hemolytic study evaluates the linkage between RBCs and developed formulations to scrutinize hemotoxicity, if any. The concentration-dependent hemolytic results figured that the effect of LA-BSA NPs followed by GEM-LA-BSA NPs have minimal hemotoxicity i.e. 1.99 \pm 0.09% and 7.36 \pm 0.37%, respectively; at 100 μ g/mL concentration. The conjugate formation

probably has no free terminal charge, causing reduced hemolytic effect. Whereas, GEM-BSA NPs exhibits maximal hemolysis i.e. $22.85 \pm 1.14\%$ at $100 \mu\text{g/mL}$ followed by BSA NPs exhibits $10.06 \pm 0.50\%$ hemolysis (**Figure 8**). Thus, it was observed that the developed formulation (GEM-LA-BSA NPs) has significantly reduced hemolytic toxicity to 11.5 folds compared to GEM-BSA NPs.

a)



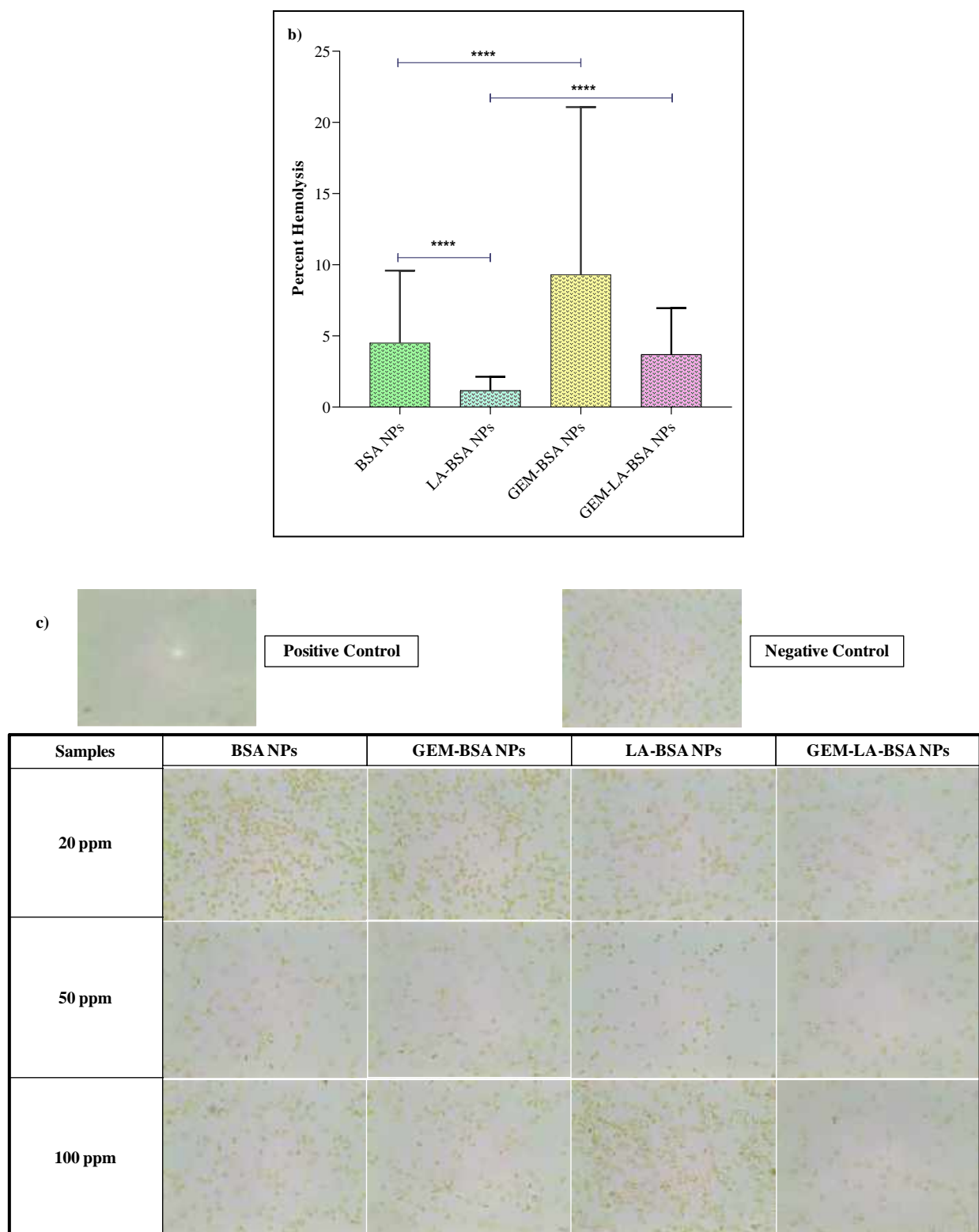
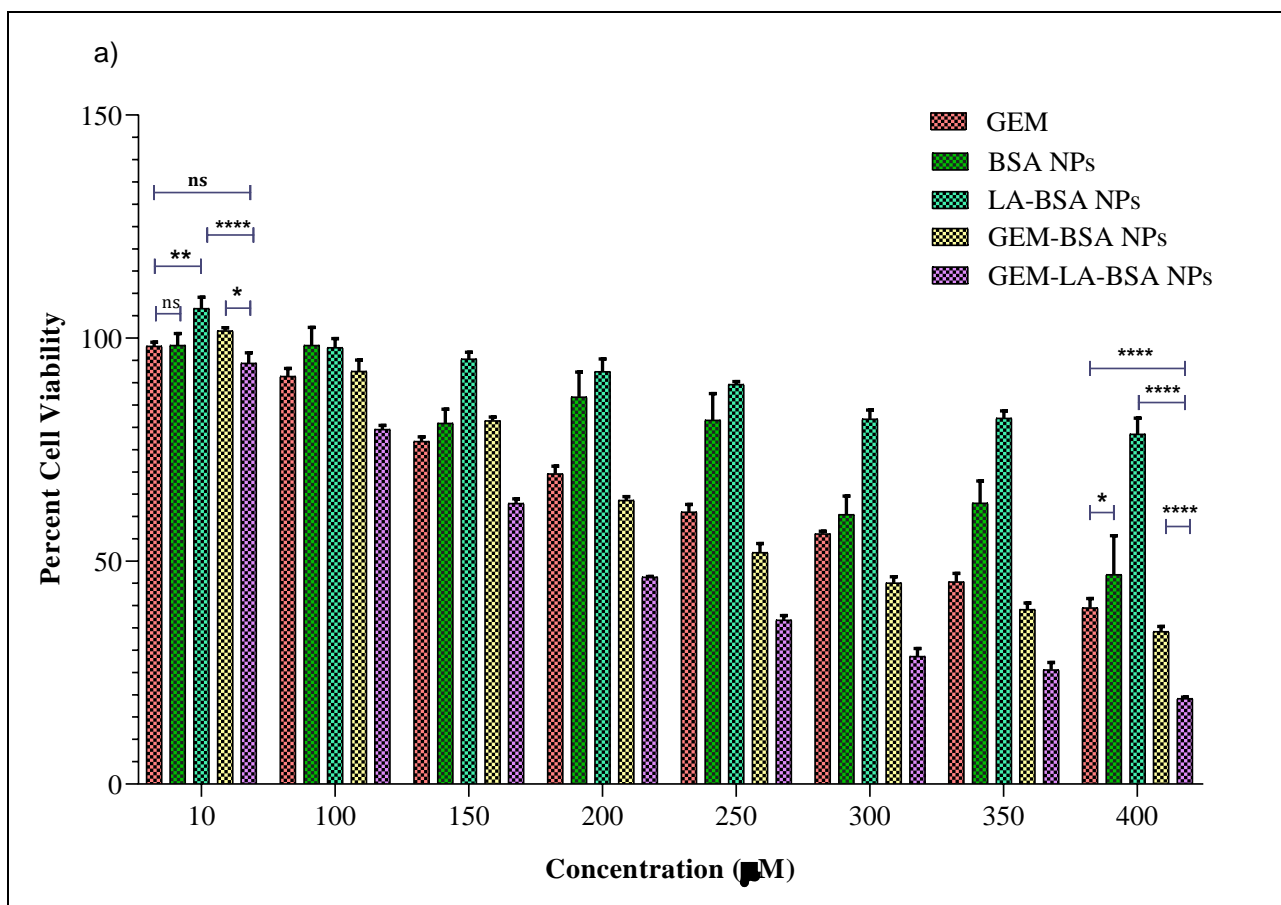


Figure 8: a) Pictorial representation of percent hemolysis through BSA NPs, LA-BSA NPs, GEM-BSA NPs, and GEM-LA-BSA NPs in different concentrations (20, 50, and 100 ppm); b)

quantitative estimation of percent hemolysis through BSA NPs, LA-BSA NPs, GEM-BSA NPs, and GEM-LA-BSA NPs in different concentrations (20, 50, and 100 ppm). *** Indicates significant difference with p value < 0.0001 ; and c) qualitative estimation of percent hemolysis through BSA NPs, LA-BSA NPs, GEM-BSA NPs, and GEM-LA-BSA NPs in different concentrations (20, 50, and 100 ppm). Values represents mean \pm SD ($n=3$).

5.8 Cell Viability and Cytotoxicity

The cell viability studies were performed on HepG2 cell lines for the determination of potency and efficacy of the prepared nanoformulations *via* MTT assay (**Figure 10**). It was observed that GEM-BSA NPs resulted in better cytotoxic effect than pure GEM with IC_{50} value of $364.03 \pm 18.20 \mu\text{g/mL}$ and $366.03 \pm 11.93 \mu\text{g/mL}$. While, the developed formulation (GEM-LA-BSA NPs) exhibited highest cytotoxic effect against HepG2 cell lines, the IC_{50} value was found to be $226.42 \pm 11.32 \mu\text{g/mL}$ and LA-BSA NPs showcased least cytotoxicity with IC_{50} value to be $871.43 \pm 44.50 \mu\text{g/mL}$ (**Figure 9**). The developed formulation could reduce the IC_{50} values by almost 40% as compared to GEM-BSA NPs.



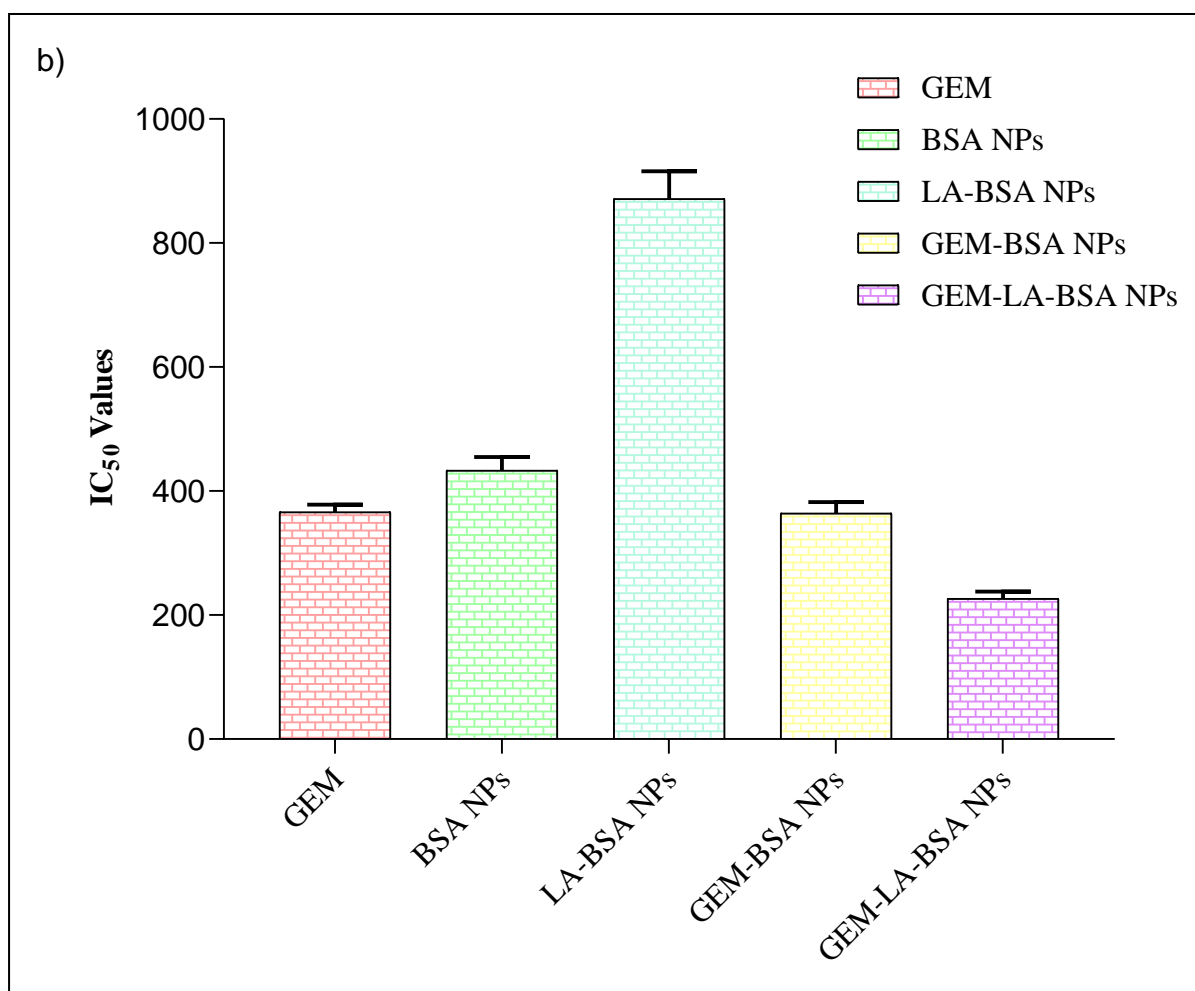


Figure 9: a) Graph representing percentage cell viability vs. concentration (μM) of GEM, BSA NPs, LA-BSA NPs, GEM-BSA NPs, and GEM-LA-BSA NPs against HepG2 cell lines; b) comparative IC₅₀ value of free GEM, BSA NPs, LA-BSA NPs, GEM-BSA NPs, and GEM-LA-BSA NPs after 24 h. **** indicates the extremely significant difference with p value < 0.0001 , ** indicates significant difference with p value < 0.005 , * indicates significant difference with p value < 0.01 , and ns indicates non-significant value. Values represent mean \pm SD ($n=3$).

5.9 Cellular Internalization Studies

The cellular uptake of nanoformulation was analyzed for the determination of the formulation entry in the cell imparting therapeutic efficacy. Hence, the confirmation of effectiveness of the nanoformulation prepared was achieved. All the drug-loaded formulations exhibited a significant cell uptake in HepG2 cells compared to the control group (**Figure 10**). It was observed that the

FITC-tagged formulations exhibited time-dependent enhancement in cellular uptake. The developed formulation (GEM-LA-BSA NPs) exhibited higher fluorescence intensity ($27 \pm 8.00\%$) in comparison to control ($20 \pm 7.00\%$) after 2 h. The quantitative estimation of cellular uptake was supported by ImageJ software. Control group exhibited low fluorescence intensity at all the time points. However, GEM-BSA NPs exhibited significantly higher fluorescence intensity of $32.27 \pm 4.69\%$, $16.02 \pm 2.56\%$, and $41.10 \pm 16.01\%$ after 2, 4, and 6 h, respectively. GEM-LA-BSA NPs exhibited fluorescence intensity of $27 \pm 8.00\%$, $24 \pm 8.00\%$, and $14 \pm 3.00\%$ after 2, 4, and 6 h, respectively. While, LA-BSA NPs exhibited lower fluorescence intensity of $24.56 \pm 7.97\%$, $8.37 \pm 2.66\%$, and $8.38 \pm 1.00\%$ after 2, 4, and 6 h, respectively than BSA NPs. BSA NPs exhibited fluorescence intensity of $20 \pm 7.00\%$, $11 \pm 1.00\%$, and $17 \pm 2.00\%$ after 2, 4, and 6 h, respectively. Thus, GEM-BSA NPs exhibited maximum cellular internalization followed by GEM-LA-BSA NPs (depicted in **figure 11**).





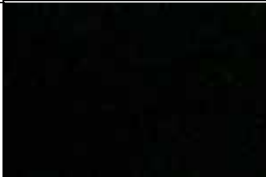



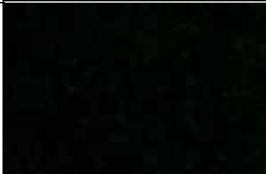
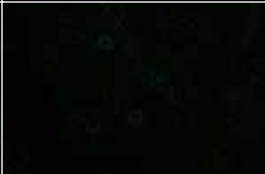


Time(h)	Control		GEM-LA-BSA-NPs	
	10X	40X	10X	40X
2				
4				
6				

Figure 10: Qualitative estimation of cellular internalization of FITC in control and GEM-LA-BSA NPs in different time intervals (2, 4, and 6 h). (10X and 40X)

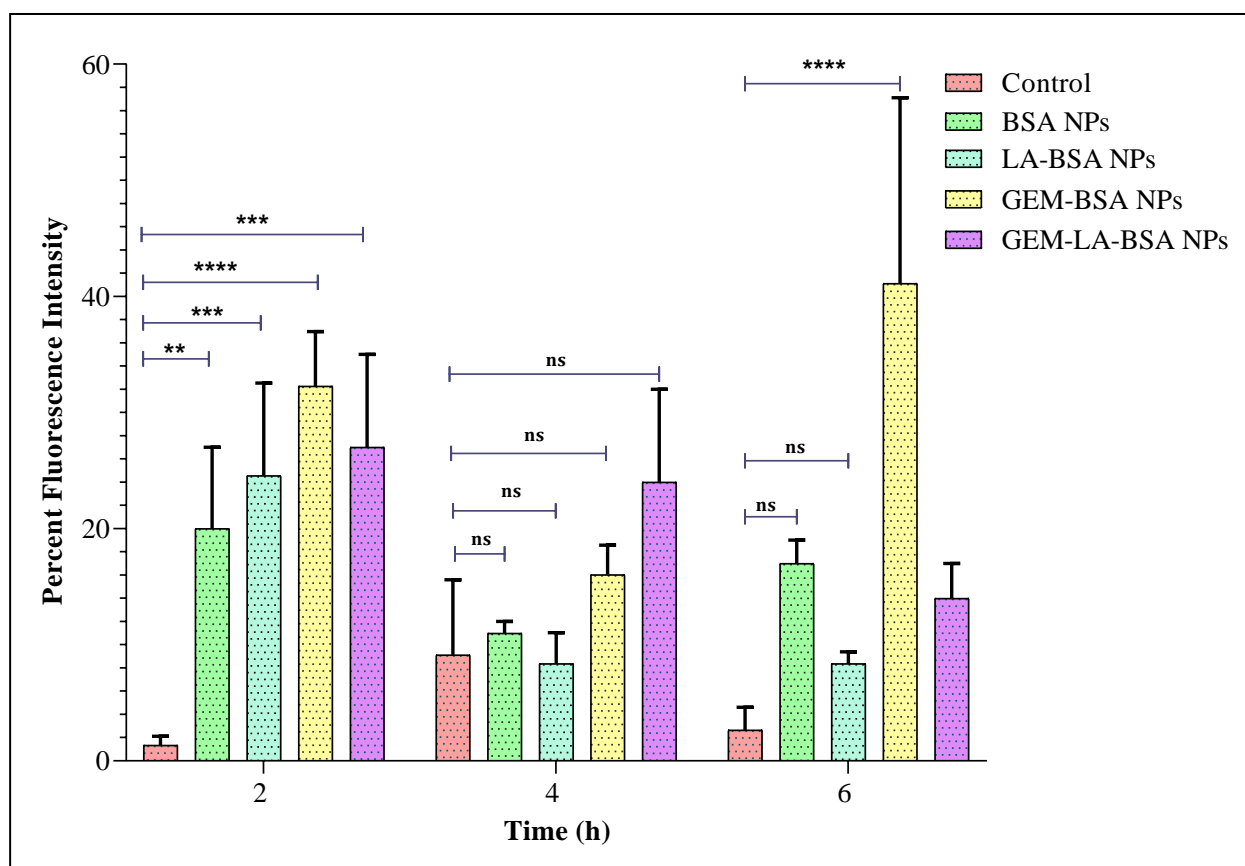


Figure 11: Quantitative estimation of cellular internalization of FITC in GEM-LA-BSA NPs, GEM-BSA NPs, LA-BSA NPs, and BSA NPs against HepG2 cell lines at 2, 4, and 6 h. **** Indicates significant difference with p value < 0.0001 , *** indicates the extremely significant difference with p value < 0.0005 and ** indicates significant difference with p value < 0.01 , and ns indicates non-significant value. Values represents mean \pm SD (n=3).

5.10 Pharmacokinetic Studies

The samples withdrawn from the Sprague Dawley rats were evaluated and analyzed using HPLC for GEM content (Huang et al., 2018)³¹. Pharmacokinetic profile revealed that pure drug (GEM) exhibit decreased plasma concentration in comparison to the GEM-loaded formulations (GEM-BSA NPs and GEM-LA-BSA NPs) over the period of 24 h (Figure 12). One compartmental open body (1 CBM) i.v. push model was utilized for the estimation of the desired pharmacokinetic parameters (Table 6). The bioavailability ($AUC_{0-\infty}$) of GEM-LA-BSA NPs was observed to be doubled the pure GEM and 1.14 times than the GEM-BSA NPs, which is

significantly higher. GEM-BSA NPs hiked 1.12 folds half-life and 1.13 folds volume of distribution (13.49 ± 0.036 and 0.0080 ± 0.0003 L) than GEM-LA-BSA NPs (12.04 ± 0.046 h and 0.0061 ± 0.0007 L, respectively) (**Table 6**). The increased volume of distribution signifies the enhanced distribution of drugs into other body tissues, leading to reduced targetability. Thus, the improved bioavailability and half-life with reduced volume of distribution and clearance rate validates the augmentation in the retention time of the formulations. Also, pharmacokinetic parameters of GEM-LA-BSA NPs were observed to be better than GEM.

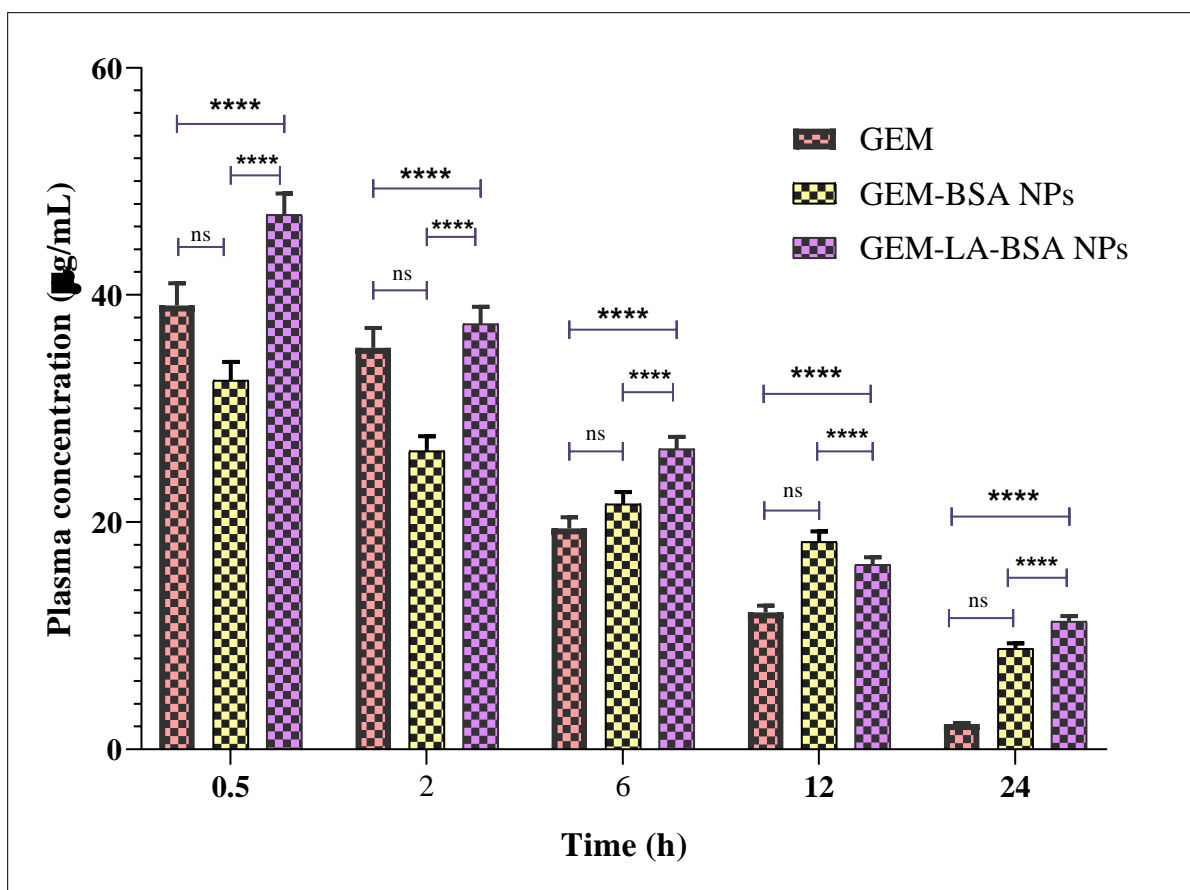


Figure 12: Plasma concentration-time profile as obtained from *in vivo* pharmacokinetic study in Sprague-Dawley rats. **** Indicates significant difference with p value < 0.0001 and ns indicates non-significant value. Values represents mean \pm SD (n=3).

Table 6: Pharmacokinetic parameters obtained from plasma concentration–time profile. Values represents mean \pm SD (n=4).

Parameters	GEM	GEM-BSA NPs	GEM-LA-BSA NPs
K_{el} (h^{-1})	0.122 \pm 0.004	0.051 \pm 0.001	0.058 \pm 0.003
$t_{1/2}$ (h)	5.68 \pm 0.027	13.49 \pm 0.036	12.04 \pm 0.046
V_d (L)	0.0054 \pm 0.0008	0.0080 \pm 0.0003	0.0061 \pm 0.0007
Cl ($L.h^{-1}$)	0.0007 \pm 0.00001	0.0004 \pm 0.00002	0.0003 \pm 0.00001
AUC _(0 to t) ($\mu g mL^{-1} h^{-1}$)	368.79 \pm 28.44	422.16 \pm 8.33	484.22 \pm 28.21
AUC _(0 to ∞) ($\mu g mL^{-1} h^{-1}$)	386.99 \pm 15.48	594.97 \pm 17.89	679.91 \pm 20.40

Here, **AUC** (0 to ∞) denotes the area under curve (bioavailability), **K_{el}** denotes elimination rate constant, **t_{1/2}** denotes the half-life, **V_d** denotes volume of distribution, and **Cl** denotes clearance of drug from the body.

6. STATISTICAL ANALYSIS

The statistical analysis results were obtained by using the Design Expert 13.0 software (Trial version 13.0, Stat-Ease Inc., Minneapolis, MN, USA) and GraphPad Prism 8.0 software (GraphPad, SanDiego, CA, USA). The regression analysis was observed to assess the statistical significance of all the developed formulations. A p -value < 0.0005 (****) was considered to be highly significant than $p < 0.01$ (*), $p < 0.01$ (**), and $p < 0.0001$ (***)).

7. DISCUSSION

LA-BSA conjugates were successfully synthesized using carbodiimide chemistry. It was characterized by TLC using 20% DCM:MeOH as a mobile phase, FT-IR spectroscopy, and confirmed by 1H -NMR spectroscopy using d-DMSO as the solvent. Galactosylated albumin-based nanoparticles (GEM-LA-BSA NPs) were prepared by the modified desolvation method. The concentrations of GEM and LA-BSA conjugates were the limiting factors of the reaction. Also, the change in the stirring speed, speed of ethanol injection, temperature, and pH were affecting the formulation of NPs. The addition of cross-linking agent, glutaraldehyde affects the transparency of the formulation. 0.1% (v/v) glutaraldehyde helps to increase the drug loading and entrapment efficiency of the NPs. Furthermore, an increase in the concentration of glutaraldehyde to 25% (v/v) leads to the formation of aggregates of a colloidal system. Thus,

optimized concentrations of the GEM:LA-BSA conjugates were required for the preparation of GEM-LA-BSA NPs. The optimization of the formulation was carried out by the Central Composite Design in the Design Expert 13.0 software. For the optimization of GEM-LA-BSA NPs, the CCD approach incorporated two independent variables (X1: wt. of GEM (mg) and X2: wt. of LA-BSA conjugate (% w/v)). A total of nine batches considering three coded levels -1 , 0 , and $+1$ with an alpha value (0.05) were generated by the design. ANOVA was introduced for the determination of the effect on response variables (Y1, Y2 and Y3) by independent variables (X1 and X2). These response variables were analyzed and fitted to different models like linear, quadratic, or 2-FI (two-factor interaction). The selection of a suitable model was carried out by determining the highest correlation coefficient value (**Table 2**). On the basis of a significant p-value and sum of squares from sequential model, the best fit model was selected for each response. The 2-FI model was observed to be the best fit for all the response variables i.e. particle size, drug loading, and entrapment efficiency. Therefore, the 2-FI model was acclaimed to elucidate the effects of the variables.

Further, the physiological characterization of the optimized formulation was preceded in comparison to the BSA NPs, GEM-BSA NPs, and LA-BSA NPs. The BSA NPs and GEM-BSA NPs seem to be spherical in shape exhibiting a nanometric size range. However, LA-BSA NPs seems to have a double layered spherical shaped morphology exhibiting highly negative charge. The outer crust reflects the presence of lactobionic acid (LA), while GEM-LA-BSA NPs were observed as agglomerate which illustrates the strong network of nanoparticles. In addition, the particle size also indicates that GEM-LA-BSA NPs exhibits larger surface area than other prepared formulations. The observed zeta potential of LA-BSA NPs and GEM-LA-BSA NPs exhibits an anionic surface charge which leads to the double layer formation and agglomerates formation, respectively.

Galactosylated-albumin nanoparticles released GEM in a sustained manner for 48 h. The nanoparticulate approach assist in bypassing burst release of drug and galactosylation helps in effective targeting of the drug. Thus, galactosylation of nanoparticles plays a pivotal role in enhancing biocompatibility of the nanocarrier. It assists in the reduction of lysis of RBC. The negligible hemolysis may assist in promoting the *in-vitro* efficacy evaluation.

The cytotoxic studies suggested that GEM-LA-BSA NPs imparted minimal cell viability against HepG2 cell lines. The cell inhibition rate of galactosylated albumin based nanoparticles

was significantly higher than the pure drug. With the increased number of an effective targeting ligand, galactose moiety in the nanoformulation would lead to the increased targetability of nanoformulation followed by site-specific drug release. This may exhibit increased cytotoxic effect against HepG2 cell lines.

The cellular internalization of GEM-LA-BSA NPs demonstrated that the presence of galactose moiety assist in facilitation of cell endocytosis in HepG2 cell lines. Thus, galactosylated albumin based nanoparticles displayed improved permeability and enhanced cell uptake *via* ASGPR-mediated cell endocytosis. It resulted into decreased cell uptake of galactosylated albumin nanoformulation (GEM-LA-BSA NPs) than GEM-BSA NPs due to competitive binding of free galactose on the ASGPR receptors.

The pharmacokinetic profile obtained could be correlated with the *in-vitro* studies. It was observed that galactosylated albumin nanoparticles would result in improved bioavailability and half-life of the encapsulated drug. With the improved targetability, it was observed that volume of distribution gradually declines and potentiates the efficacy of LA-BSA towards ASGP receptors

8. IMPACT OF THE RESEARCH IN THE ADVANCEMENT OF KNOWLEDGE OR BENEFIT TO MANKIND

Gemcitabine loaded galactosylated nanoparticles (GEM-LA-BSA NPs) were evaluated to improve site-specific targeting and the overall therapeutic efficacy of GEM against hepatocellular carcinoma (HCC). The concept of galactosylation has been utilized for the effective ASGPR targeting and enhances drug encapsulation leading to the enhanced bioavailability of GEM. These improved properties assist the drug in the malignant hepatocytes. The developed GEM-LA-BSA NPs were optimized using design expert 13.0 software (Central Composite Design). The optimized formulation confirmed the biocompatible nature of GEM-LA-BSA NPs by hemolytic studies demonstrating minimal erythrocytes rupture. The *in-vitro* studies exhibit reduced cell viability of GEM-LA-BSA NPs against HepG2 cells, resulting in minimal inhibitory concentration in comparison to free drug. *In-vivo* pharmacokinetic studies confirm the improved bioavailability and half-life of GEM, demonstrating chemopreventive and therapeutic effect against HCC.

Taken together, the results manifest the potential of LA-BSA conjugates in the targeting of ASGPR receptors on hepatocytes for the effective drug delivery of small molecular anti-cancer drugs. Further exploration of galactosylation albumin nanoparticles can be evaluated in suitable tumor model as well as the formulation batch can be planned for larger quantity to establish the robustness of the methodology.

9. LITERATURE REFERENCES

- (1) **WHO Report, 2020.** <https://gco.iarc.fr/today/fact-sheets-cancers>. <https://doi.org/10.3322/caac.21492>. (accessed on 07-05-2023).
- (2) Morell, A. G.; Irvine, R. A.; Sternlieb, I.; Scheinberg, I. H.; Ashwell, G. Physical and chemical studies on ceruloplasmin: v. metabolic studies on sialic acid-free ceruloplasmin *in vivo*. *J. Biol. Chem.* **1968**, *243* (1), 155–159. [https://doi.org/10.1016/S0021-9258\(18\)99337-3](https://doi.org/10.1016/S0021-9258(18)99337-3).
- (3) O'Hare, K. B.; Hume, I. C.; Scarlett, L.; Chytrý, V.; Kopečarková, P.; Kopeček, J.; Duncan, R. Effect of galactose on interaction of n-(2-hydroxypropyl)methacrylamide copolymers with hepatoma cells in culture: Preliminary application to an anticancer agent, Daunomycin. *Hepatology* **1989**, *10* (2), 207–214. <https://doi.org/10.1002/HEP.1840100215>.
- (4) **FDA-NDA Review and Evaluation, 2011.** https://www.accessdata.fda.gov/drugsatfda_docs/nda/2011/022434Orig1s000PharmR.pdf. (accessed on 07-05-2023).
- (5) Pan, Q.; Lv, Y.; Williams, G. R.; Tao, L.; Yang, H.; Li, H.; Zhu, L. Lactobionic acid and carboxymethyl chitosan functionalized graphene oxide nanocomposites as targeted anticancer drug delivery systems. *Carbohydr. Polym.* **2016**, *151*, 812–820. <https://doi.org/10.1016/J.CARBPOL.2016.06.024>.
- (6) Ruman, U.; Fakurazi, S.; Masarudin, M. J.; Hussein, M. Z. Nanocarrier-based therapeutics and theranostics drug delivery systems for next generation of liver cancer nanodrug modalities. *Int. J. Nanomed.* **2020**, *15*, 1437–1456. <https://doi.org/10.2147/IJN.S236927>.
- (7) Bayda, S.; Adeel, M.; Tuccinardi, T.; Cordani, M.; Rizzolio, F. The history of nanoscience and nanotechnology: From chemical–physical applications to nanomedicine. *Molecules* **2019**, *25* (1), 112. <https://doi.org/10.3390/MOLECULES25010112>.

- (8) American Biosciences, Inc. ABRAXANE® for injectable suspension (paclitaxel protein-bound particles for injectable suspension) (albumin-bound). 21660, 2013. www.fda.gov/medwatch. (accessed 2023-05-07).
- (9) Wang, J.; Zhang, B. Bovine serum albumin as a versatile platform for cancer imaging and therapy. *Curr. Med. Chem.* **2018**, *25* (25), 2938–2953. <https://doi.org/10.2174/0929867324666170314143335>.
- (10) Song, X.; Liang, C.; Gong, H.; Chen, Q.; Wang, C.; Liu, Z. Photosensitizer-conjugated albumin–polypyrrole nanoparticles for imaging-guided *in vivo* photodynamic/photothermal therapy. *Small* **2015**, *11* (32), 3932–3941. <https://doi.org/10.1002/SMLL.201500550>.
- (11) Kushwah, V.; Agrawal, A. K.; Dora, C. P.; Mallinson, D.; Lamprou, D. A.; Gupta, R. C.; Jain, S. Novel gemcitabine conjugated albumin nanoparticles: A potential strategy to enhance drug efficacy in pancreatic cancer treatment. *Pharm. Res.* **2017**, *34* (11), 2295–2311. <https://doi.org/10.1007/S11095-017-2238-8/FIGURES/8>.
- (12) **USFDA** **Report**, **2010**. https://www.accessdata.fda.gov/drugsatfda_docs/label/2010/020509s064lbl.pdf. (accessed on 07-05-2023).
- (13) Martín-Banderas, L.; Sáez-Fernández, E.; Holgado, M. Á.; Durán-Lobato, M. M.; Prados, J. C.; Melguizo, C.; Arias, J. L. Biocompatible gemcitabine-based nanomedicine engineered by flow focusing® for efficient antitumor activity. *Int. J. Pharm.* **2013**, *443* (1–2), 103–109. <https://doi.org/10.1016/J.IJPHARM.2012.12.048>.
- (14) Aggarwal, S.; Gupta, S.; Pabla, D.; Murthy, R. S. R. Gemcitabine-loaded PLGA-PEG immunonanoparticles for targeted chemotherapy of pancreatic cancer. *Cancer Nanotechnol.* **2013**, *4* (6), 145–157. <https://doi.org/10.1007/S12645-013-0046-3/FIGURES/9>.
- (15) Ahmed, M.; Narain, R. Carbohydrate-based materials for targeted delivery of drugs and genes to the liver. *Nanomedicine (Lond.)* **2015**, *10* (14), 2263–2288. <https://doi.org/10.2217/NNM.15.58>.
- (16) Li, C.; Zhang, D.; Guo, H.; Hao, L.; Zheng, D.; Liu, G.; Shen, J.; Tian, X.; Zhang, Q. Preparation and characterization of galactosylated bovine serum albumin nanoparticles for liver-targeted delivery of oridonin. *Int. J. Pharm.* **2013**, *448* (1), 79–86.

- <https://doi.org/10.1016/J.IJPHARM.2013.03.019>.
- (17) Thao, L. Q.; Lee, C.; Kim, B.; Lee, S.; Kim, T. H.; Kim, J. O.; Lee, E. S.; Oh, K. T.; Choi, H. G.; Yoo, S. D.; Youn, Y. S. Doxorubicin and paclitaxel co-bound lactosylated albumin nanoparticles having targetability to hepatocellular carcinoma. *Colloids Surf. B: Biointerfaces*. **2017**, *152*, 183–191. <https://doi.org/10.1016/J.COLSURFB.2017.01.017>.
 - (18) Dayani, L.; Dehghani, M.; Aghaei, M.; Taymouri, S.; Taheri, A. Preparation and evaluation of targeted albumin lipid nanoparticles with lactobionic acid for targeted drug delivery of sorafenib in hepatocellular carcinoma. *J. Drug Deliv. Sci. Technol.* **2022**, *69*, 103142. <https://doi.org/10.1016/J.JDDST.2022.103142>.
 - (19) Yalcin, T. E.; Ilbasimis-Tamer, S.; Takka, S. Development and characterization of gemcitabine hydrochloride loaded lipid polymer hybrid nanoparticles (LPHNs) using central composite design. *Int. J. Pharm.* **2018**, *548* (1), 255–262. <https://doi.org/10.1016/J.IJPHARM.2018.06.063>.
 - (20) Weber, C.; Coester, C.; Kreuter, J.; Langer, K. Desolvation process and surface characterisation of protein nanoparticles. *Int. J. Pharm.* **2000**, *194* (1), 91–102. [https://doi.org/10.1016/S0378-5173\(99\)00370-1](https://doi.org/10.1016/S0378-5173(99)00370-1).
 - (21) Khare, V.; Sakarchi, W. Al; Gupta, P. N.; Curtis, A. D. M.; Hoskins, C. Synthesis and characterization of TPGS–gemcitabine prodrug micelles for pancreatic cancer therapy. *RSC Adv.* **2016**, *6* (65), 60126–60137. <https://doi.org/10.1039/C6RA09347G>.
 - (22) Nair, A. B.; Shah, J.; Al-Dhubiab, B. E.; Patel, S. S.; Morsy, M. A.; Patel, V.; Chavda, V.; Jacob, S.; Sreeharsha, N.; Shinu, P.; Attimarad, M.; Venugopala, K. N. Development of asialoglycoprotein receptor-targeted nanoparticles for selective delivery of gemcitabine to hepatocellular carcinoma. *Molecules* **2019**, *24* (24), 4566. <https://doi.org/10.3390/MOLECULES24244566>.
 - (23) Dora, C. P.; Kushwah, V.; Katiyar, S. S.; Kumar, P.; Pillay, V.; Suresh, S.; Jain, S. Improved metabolic stability and therapeutic efficacy of a novel molecular gemcitabine phospholipid complex. *Int. J. Pharm.* **2017**, *530* (1–2), 113–127. <https://doi.org/10.1016/J.IJPHARM.2017.07.060>.
 - (24) Slowing, I. I.; Wu, C. W.; Vivero-Escoto, J. L.; Lin, V. S. Y. Mesoporous silica nanoparticles for reducing hemolytic activity towards mammalian red blood cells. *Small* **2009**, *5* (1), 57–62. <https://doi.org/10.1002/SMLL.200800926>.

- (25) Tekchandani, P.; Kurmi, B. Das; Paliwal, R.; Paliwal, S. R. Galactosylated TPGS micelles for docetaxel targeting to hepatic carcinoma: Development, characterization, and biodistribution study. *AAPS PharmSciTech* **2020**, *21* (5), 1–11. <https://doi.org/10.1208/S12249-020-01690-4/FIGURES/6>.
- (26) Mosmann, T. Rapid colorimetric assay for cellular growth and survival: Application to proliferation and cytotoxicity assays. *J. Immunol. Methods* **1983**, *65* (1–2), 55–63. [https://doi.org/10.1016/0022-1759\(83\)90303-4](https://doi.org/10.1016/0022-1759(83)90303-4).
- (27) Paul, D.; Chandrakala, P.; Surendran, S.; Bitla, P.; Satheeshkumar, N. Pharmacokinetic interaction study of novel combination of palbociclib and sorafenib for hepatocellular carcinoma in SD rats. *J. Chromatogr. B* **2019**, *1108*, 25–31. <https://doi.org/10.1016/J.JCHROMB.2019.01.003>.
- (28) Pavia, D. L.; Lampman, G. M.; Kriz, G. S. Nuclear magnetic resonance spectroscopy. In *Introduction to Spectroscopy*; Thomson Learning, Inc., 2001; pp 134–158.
- (29) Wu, L.; Zhang, J.; Watanabe, W. Physical and chemical stability of drug nanoparticles. *Adv. Drug Deliv. Rev.* **2011**, *63* (6), 456–469. <https://doi.org/10.1016/J.ADDR.2011.02.001>.
- (30) Jun, J. Y.; Nguyen, H. H.; Paik, S. Y. R.; Chun, H. S.; Kang, B. C.; Ko, S. Preparation of size-controlled bovine serum albumin (BSA) nanoparticles by a modified desolvation method. *Food Chem.* **2011**, *127* (4), 1892–1898. <https://doi.org/10.1016/J.FOODCHEM.2011.02.040>.
- (31) Huang, Y.; Hu, L.; Huang, S.; Xu, W.; Wan, J.; Wang, D.; Zheng, G.; Xia, Z. Curcumin-loaded galactosylated BSA nanoparticles as targeted drug delivery carriers inhibit hepatocellular carcinoma cell proliferation and migration. *Int. J. Nanomed.* **2018**, *13*, 8309. <https://doi.org/10.2147/IJN.S184379>.

Sanya Batheja